

学位論文

**The Processes of the Thermal and Material
Evolution of a Magma System in a Crust**

地殻内のマグマシステムにおける熱物質進化過程

平成7年12月 博士（理学）申請

東京大学大学院理学系研究科
地質学専攻

金子克哉

The Processes of the Thermal and Material Evolution of a Magma System in a Crust

Katsuya KANEKO

University of Tokyo

December 1995

Abstract

The purpose in this thesis is to elucidate the physical processes governing the thermal and compositional evolution of a magma and a continental crust surrounding it from view points of the thermal and mass balances between the magma and the crust. I refer to the system that consists of the magma and the surrounding crust as "the magma system" in this thesis. Since the temperature of a magma from the mantle is near or equal to its liquidus and is commonly higher than the melting temperature of the crust, the mass and energy balances in the magma system are governed by complex processes including simultaneous melting and crystallization. These processes are discussed based on the theoretical analyses and the results of the analogue experiments.

The thermal transfer processes between a hot liquid and a cold solid have been analyzed theoretically to understand the important factors which govern the cooling of the magma. The results indicate that when the solid/liquid interface migrates due to melting of the crust and the liquid convects vigorously, the temperature of the liquid decreases very rapidly regardless of the solid temperature, and that the liquid cools slowly in the other cases. The analyses also suggest that when the magma is convective, the relationship between the temperature of the magma (T) and the melting temperature of the crust (T_m) is the most important factor to determine the thermal history of the magma. When $T > T_m$, the magma decreases in temperature rapidly and the crust melts (the rapid cooling stage). On the other hand, when $T < T_m$, the magma cannot melt the crust and the temperature of the magma decreases slowly (the slow cooling stage).

Analogue experiments have been carried out using a saturated NH_4Cl aqueous solution and the solid mixture with eutectic composition in the NH_4Cl - H_2O binary eutectic system to consider the condition under which the melting and/or crystallization occur at the roof and the floor of the magma chamber. When a cold solid mixture with the eutectic composition is placed at the top of a hot solution of higher NH_4Cl content, vigorous thermal convection occurs in the solution, which results in rapid melting of the solid roof to form a stable melt layer with negligible mixing of the underlying liquid. On

the other hand, when the cold solid mixture is placed at the bottom of the hot solution, the convection is driven by compositional instabilities due to floor melting as well as crystallization just above the floor. Because the compositional convection carries a low heat flux, the rate of melting and the temperature profiles around the floor do not differ greatly from those that would be observed due to conduction alone. Unlike the roof melting, the melt generated by the floor melting efficiently mixes with the overlying solution. The compositional gradient generated by the compositional convection enhances the formation of the double-diffusive convective layers and decreases the upward heat flux indirectly.

Another series of analogue experiments has been carried out to understand the effects of the compositional and the temperature variation of the floor crust on the evolution of the magma system. The NH_4Cl contents and the initial temperatures of the solid mixtures were systematically changed in the experiments. As the NH_4Cl content of the solid becomes higher, the rate of the compositional differentiation of the liquid decreases. This can be explained by two mechanisms. (1) As the NH_4Cl content of the solid becomes higher, the melting degree of the solid at the solidus becomes smaller and hence the latent heat required by the migration of the interface between the solid and partially molten zone (mush) decreases. Thus, the interface migration becomes faster and hence the temperature gradient just above the interface becomes smaller. These effects result in low heat flux from the mush to the interface and decrease the production rate of the melt with low NH_4Cl content. (2) As the NH_4Cl content of the solid becomes higher, the permeability of the mush becomes smaller. Thus, compositional convection induced by the instability in the mush becomes less vigorous and the liquid of the low NH_4Cl content mixes with the overlying solution less effectively. On the other hand, as the initial temperature of the solid became colder, the rate of the compositional differentiation of the liquid decreases. This is because as the initial temperature of the solid became colder, the heat loss into the solid increases and hence the production rate of the melt of the low NH_4Cl content decreases.

The implication for the thermal and compositional evolution of a magma system is that, when a basaltic magma is emplaced in the continental crust, a silicic magma is rapidly formed by the roof melting, and that the magmas evolve very slowly after the temperatures of the magmas become as cool as the melting temperature of the crust. The major effects of the floor melting would be that the liquid line of descent of the basaltic magma can be greatly modified by mixing with the melt generated at the floor and the interstitial liquid in the mush and that the upward heat flux decreases due to the formation of the double-diffusive layers. When the magma system evolves in this scenario, the variations of the temperature and composition of the crust would affect the evolution of the magma system in the following four points. (i) The temperature of the roof crust gives little effect on the rate of the temperature decrease of the magma in the rapid cooling stage but changes the amount of the melt generated by melting of the roof crust and the cooling of the magma in the slow cooling stage. As the temperature of the roof crust is colder, the amount of the melt generated by roof melting of the crust decreases and the time scale of solidification of the magma becomes shorter. (ii) As the melting temperature of the roof crust becomes higher due to the change in compositions, the transition of the rapid and the slow cooling stages occurs at a higher temperature of the magma. (iii) As the temperature of the floor crust is colder, the amount of the melt generated by melting of the floor crust decreases and hence the rate of the compositional differentiation of the basaltic magma decreases. (iv) When the composition of the floor crust changes, change of its melting temperature and/or change of the degree of partial melting of the crust at the constant melting temperature occur. As the melting temperature of the floor crust becomes higher or as the degree of the partial melting of the crust decreases, then the amount of the melt generated by melting of the floor crust decreases in both cases and the compositional convection becomes less vigorous in the latter case. Therefore, the rate of the compositional differentiation of the basaltic magma decreases.

Contents

1. Introduction	1
2. Theoretical Analysis on the Thermal History of a Magma System	5
2.1. Thermal balance at the moving interface between the solid and liquid	5
2.2. Numerical calculations in the one dimensional model	8
2.3. Summary	11
Tables and figures	13
3. Analogue Experiments. Part 1 : Melting and Crystallization at the Interfaces between the Liquid and the Overlying and/or Underlying Solid	21
3.1. Experimental technique and conditions	22
3.2. The roof experiment	24
3.3. The floor experiment	28
3.4. The both sides experiment	34
3.5. Comparisons of the results of three experiments	39
3.6. Summary	40
Tables and figures	42
Plates	73
4. Analogue Experiments. Part 2 : The Effects of the Composition and the Temperature of the Solid below the Liquid	79
4.1. Experimental technique and conditions	79
4.2. The effect of the composition of the solid	80
4.3. The effect of the initial temperature of the solid	83
4.4. Summary	84
Tables and figures	86

Plates	102
5. Implication to a Natural Magma System	104
5.1. The evolution of the magma system for a single intrusive event	104
5.2. The effects of the temperature and compositional variation of the crust	107
Figures	111
6. Concluding Remarks	117
7. Acknowledgments	121
8. References	122

List of Figures

Fig.2-1. Geometry near the solid/liquid interface.

Fig.2-2. The migration of the solid/liquid interface and the temperature profile.

Fig.2-3. Definition sketches for the analysis of §2.2.

Fig.2-4. Results of the numerical calculation §2.2 in the Case 1, 2, and 3.

Fig.2-5. The time period of cooling versus the initial liquid thickness.

Fig.2-6. The schematic diagram showing the change of the temperature of the magma with time by the set of the EFTs of the crust and the magma.

Fig.3-1. The mechanisms of convection at the roof and the floor of the magma chamber

Fig.3-2. The phase diagram of the $\text{NH}_4\text{Cl-H}_2\text{O}$ system.

Fig.3-3. Geometry of the three experiments.

Fig. 3-4. Experimental apparatus.

Fig.3-5. The schematic sketch of the roof experiment.

Fig.3-6. The change of the interface positions in the roof experiment.

Fig.3-7. The change of the temperature measured at the fixed position in the roof experiment.

Fig.3-8. The Rayleigh number of the upper and the lower liquid layers.

Fig.3-9. Diagram showing the various forms of convection observed in a horizontal layer of liquid, as a function of Rayleigh and Prandtl numbers (Krishnamurti, 1970a,b).

Fig.3-10. Temperature and liquidus profiles in the roof experiment.

Fig.3-11. The change of the solid front in the roof experiment.

Fig.3-12. The heat flux to the solid front from the upper liquid layer versus the difference between the temperatures of the upper liquid layer and the eutectic temperature.

Fig.3-13. The schematic sketches of the floor experiment.

Fig.3-14. Change of the interface positions and the mush thickness in the floor experiment.

Fig.3-15. Temperature and liquidus profiles in the floor experiment.

Fig.3-16. Change of the liquid compositions in the floor experiment.

Fig.3-17. Schematic sketches on the migration of the mush front.

Fig.3-18. Change of the solid front in the floor experiment.

Fig.3-19. Change of temperature profiles in the floor experiment and predicted in the diffusion model.

Fig.3-20. The schematic sketches of the both sides experiment.

Fig.3-21. Change of the interface positions in the both sides experiment.

Fig.3-22. The change of the temperature measured at the fixed position in the both sides experiment.

Fig.3-23. Change of the liquid compositions in the both sides experiment.

Fig.3-24. Temperature and liquidus profiles in the both sides experiment.

Fig.3-24. Change of the temperature and the composition of the upper and the lower liquid layers on the phase diagram.

Fig.3-25. Schematic sketch of change of the temperature and the composition of the upper and the lower liquid layers.

Fig.3-26. Changes of the interface in all experiments.

Fig.3-27. Temperature profiles in all experiments.

Fig.4-1. The initial conditions of the experiments in §4.2 and §4.3 on the phase diagram.

Fig.4-2. Schematic sketches of the observation in the experiments of 28 wt% solid.

Fig.4-3. Change of the bulk compositional profile in the experiment of 73 wt% solid.

Fig.4-4. Change of the solid and the mush fronts and the mush thickness in the experiments in §4.2.

Fig.4-5. Change of the average liquid composition and the compositional profiles in the experiments in §4.2.

Fig.4-6. Temperature and liquidus profiles in the experiment of 28wt% solid.

Fig.4-7. Temperature and liquidus profiles in the experiment of 73wt% solid.

Fig.4-8. Temperature profiles in the experiments of the eutectic, 28wt% and 73wt% solid.

Fig.4-9. Change of the downward heat flux at the solid front.

Fig.4-10. Change of the compositional flux in the experiments in §4.2.

Fig.4-11. The migration of the solid front and the temperature gradient above the solid front.

Fig.4-12. Change of the solid and the mush fronts and the mush thickness in the experiments in §4.3.

Fig.4-13. Change of the average liquid composition and the compositional profiles in the experiments in §4.3.

Fig.4-14. Temperature and liquidus profiles in the experiment of cold solid.

Fig.4-15. Temperature profiles in the experiments of the warm and the cold solids.

Fig. 5-1. The change of the time period of the rapid cooling stage due to the formation of the double-diffusive layers in the magma.

Fig.5-2. The effects of the various temperature of the roof crust.

Fig.5-3. The effects of the various composition of the roof crust.

Fig.5-4. The effects of the various temperature of the floor crust.

Fig.5-5. Calculation results of the migration of the solid/liquid interface in the model of Case 2 in §2.

Fig.5-6. The effects of the various temperature of the floor crust.

List of Tables

Table 2-1. Parameter value in the calculation

Table 2-2. Properties of the rapid cooling stage and the slow cooling stage

Table 3-1. Parameter values of the experimental system.

Table 3-2. List of the experiments and their initial conditions in §3

Table 4-1. List of the experiments and their initial conditions in §4

Table 4-2. The solid fraction at the eutectic temperature

List of Plates

Plate.3-1. Immediately after the roof experiment started.

Plate.3-2. Shadow graph at 10 min in the roof experiment.

Plate.3-3. The roof experiment at 120 min.

Plate.3-4. Immediately after the floor experiment started.

Plate.3-5. The floor experiment at 120 min.

Plate.3-6. Shadow graph at 120 min in the floor experiment.

Plate.3-7. Immediately after the both sides experiment started.

Plate.3-8. Shadow graph at 15 min in the both sides experiment.

Plate.3-9. The both sides experiment at 80 min.

Plate.3-10. Shadow graph at 160 min in the both sides experiment.

Plate.3-11. Shadow graph at 260 min in the both sides experiment.

Plate.4-1. The experiment using 28 wt% floor solid at 120 min.

Plate.4-2. Shadow graph at 120 min in the experiment using 28 wt% floor solid.

Plate.4-3. The experiment using 73 wt% floor solid at 120 min.

Plate.4-4. Shadow graph at 120 min in the experiment using 73 wt% floor solid.

1. Introduction

A magma generated in the Earth's mantle differentiates in a magma chamber in a crust. Divergent features of erupting magmas are determined by the processes of the thermal and compositional evolution in the crust (e.g. Turner and Campbell, 1986). Classical methods of petrology based on the equilibrium relations between phases allow us to estimate the pressure and the temperature at which generation or fractionation of the magma occurs. They, however, do not enable us to fully understand the mechanisms that determine the temperature and the composition of the erupting magmas, because they give only the relationship between the intensive parameters such as pressures, temperatures, and compositions, but do not tell anything about the energy balance between the magma and the crust.

The fundamental aim of this thesis is to elucidate the physical processes governing the thermal and compositional evolution of the magma in the crust from view points of both the mass and energy balances between magma and crust. I refer to the system that consists of both the magma and the crust surrounding it as "the magma system" in this thesis. One of the most important characteristics of the magma system is that when a new magma is supplied into the magma system, the temperature of the magma is near or equal to its liquidus and is commonly higher than solidus of a continental crust. Therefore, the mass and energy balances in the magma system are governed by complex processes including simultaneous crystallization and melting.

One of the proper approaches to understand such complex processes would be experimental one in the analogous system. In order that the analogous system simulates the natural magma system, the system should include melting and crystallization processes and the melt generated by melting and the residual liquid due to crystallization is positively buoyant (e.g. Jaupart and Tait, 1995). In the previous studies, the heat transfer and the liquid motion induced by melting and/or crystallization have been investigated experimentally using the analogous system having the above nature. I briefly

review these previous studies and the related theoretical studies on the processes at the top or the bottom of the liquid in the following two paragraphs.

There are two important previous studies on the processes at the top of the liquid, which are Campbell and Turner (1987) and Huppert and Sparks (1988a,b). Campbell and Turner (1987) experimentally investigated melting of the roof solid and crystallization of the liquid. They observed the formation of two separate layers of the molten solid and the original liquid, both of which began to convect thermally. Huppert and Sparks (1988a,b) experimentally investigated melting of the roof solid and observed basically the same phenomena as Campbell and Turner (1987). Huppert and Sparks (1988a, b) developed the theoretical model on this system and clarified that the melting of the roof solid accompanying migration of the solid/liquid interface proceeds very rapidly and that the rate of the temperature decrease of the liquid in this case is much larger than the case in which no melting of the roof solid occurs.

The phenomena at the bottom of the liquid are very different from those at the top. Either melting or crystallization at the bottom of the liquid has been studied previously. Campbell (1986), Woods (1991) and Kerr (1994) experimentally and theoretically investigated melting processes at the bottom of the liquid which does not crystallize. They found that the light molten solid induces compositional convection and mixes with the overlying liquid, and that the heat flux carried by the compositional convection depends on the density difference between the molten solid and the overlying liquid. On the other hand, Tait and Jaupart (1989, 1992), Chen and Chen (1991) and Chen et al. (1993) experimentally investigated crystallization processes of the liquid cooled from below. They all observed the formation of the mush where solid and liquid coexist at the bottom of the liquid and two modes of the compositional convection: one is driven by buoyant residual liquid within the mush and the other is associated with the thin compositional boundary layer in the melt just above the mush surface, both of which are possible theoretically (Worster, 1992). Compositional convection induced by these instabilities carries a low heat flux under some conditions (e.g. Jaupart and Tait, 1995), but it carries heat flux efficiently under other condition (e.g. Kerr, 1994).

The above reviews of the previous work suggest that there remain at least four fundamental problems to understand the whole thermal and compositional evolution of the solid-liquid system. First, Huppert and Sparks (1988a,b) did not cover all cases of migrations of the liquid/solid interface and convective states of the liquid that might occur in the natural system. Second, the system in which simultaneous melting and crystallization occur at the bottom of the liquid has not been investigated in the previous studies. Third, the interaction between the processes at the top and bottom interfaces of the liquid is not understood. The natural magma system has both interfaces. The interaction between the processes at both interfaces may significantly change the heat transfer and the liquid motion of the magma system. Fourth, there is no previous experimental study in which the solid composition was changed systematically. The solid composition determines its solidus and liquidus and the melting degree at some temperature. Thus, the change of the solid composition is expected to change the temperature at the solid/liquid interface and the amount and the composition of the melt generated by melting of the solid.

In this thesis, I tackled the above four problems in the following three chapters on the basis of the results of the theoretical analysis and the analogue experiments using a hot, NH_4Cl aqueous solution and a cold solid mixture of ice and NH_4Cl .

In §2, theoretical analyses on the heat transfer processes between a hot liquid and a cold solid are presented. I consider various sets of the melting temperatures of the solid and the liquid and the case in which the liquid is convective or not. From the results of the theoretical analysis, it is emphasized that a set of the crustal melting temperature and the magmatic temperature is the most important to the thermal history of the magma system and that the magma system has the two cooling stages of very different time scales.

In §3, I attempt to give some solutions to the second and third problems. The heat transfer at the solid/liquid interface and the liquid motion of the system are discussed using the results of the three analogue experiments in which the liquids were in contact with the solids at the top of the liquid, at the bottom, or at both the top and bottom. The

results of the experiments indicate that the processes at each interface give very different effects on the evolution of the solid-liquid system. Their interactions are discussed based on the results of the three experiments.

In §4, I attempt to give some solutions to the fourth problem. The analogue experiments in which the liquids were in contact with the solids with various compositions and temperatures at the bottom of the liquid. The results indicate that the evolution of the system systematically changes, for example, in terms of the rate of the melting and the compositional differentiation, as the composition and the temperature of the solid change. The mechanisms of these systematic changes are considered.

In §5, I consider the thermal and compositional evolution of the natural magma system and its time scale on the basis of all theoretical and experimental results.

2. Theoretical analyses on the thermal history of a magma system

The heat transfer processes between a hot liquid and a cold solid are analyzed theoretically in this section to understand the important factors that govern the thermal history of the magma system. Huppert and Sparks (1988a, b) clarified that the melting of the roof solid accompanying migration of the solid/liquid interface proceeds very rapidly and increases the rate of the temperature decrease of the convective liquid much more than the case in which no melting of the roof solid occurs. I extend Huppert and Sparks (1988a,b) and consider the various sets of the solid and liquid with the different melting temperatures and the cases in which the liquid is convective or not.

2.1. Thermal balance at the moving interface between the solid and the liquid

Consider a one-dimensional coordinate system with the z -axis and the liquid with finite thickness in contact with the solid with semi-infinite thickness at $z=a$. The heat flux from the liquid to the solid/liquid interface F_{TL} and the heat flux from the interface to the solid F_{TS} can only be balanced by the latent heat released or absorbed due to the migration of the solid/liquid interface. Its relationship is given by

$$F_{TL} = F_{TS} + \rho L \frac{da}{dt} \quad (2-1)$$

where ρ is density and L is the heat of fusion. The second term of the right hand side is positive when the solid melts and negative when the liquid solidifies (Fig. 2-1).

The heat transfer process in a solid is only conduction so that the temperature profile is governed by the diffusion equation. Thus the heat flux from the solid/liquid interface to the solid is given by

$$F_{TS} = -k_s \left. \frac{\partial T}{\partial z} \right|_{z=a+} \quad (2-2)$$

where T is the temperature in the solid with respect to a fixed z -axis and k_s is thermal conductivity of the solid. When a cold solid is in contact with a hot liquid, F_{TS} must be

very large initially. As time proceeds, however, F_{TS} decreases rapidly as the conductive temperature profile in the solid relaxes.

The heat flux from the liquid to the solid/liquid interface in the case of the convective liquid is different from that in the case of the stagnant liquid. When the liquid is uniform in temperature due to vigorous convection, F_{TL} is given by

$$F_{TL} = \lambda k_l \left(\frac{\alpha g}{\kappa_l \nu} \right)^{1/3} (T_l - T_i)^{4/3} \quad (2-3a)$$

where T_l is the uniform liquid temperature and T_i is the temperature at the interface, and α , k_l , κ_l , ν are thermal expansion coefficient, thermal conductivity, thermal diffusivity, and kinematic viscosity of liquid, respectively. g is gravity acceleration and λ is an empirical constant (e.g. Turner, 1979). F_{TL} is independent of the thickness of the convective liquid layer and determined by the temperature difference between the internal liquid and the interface, when the unstable plumes produced continuously near the cold interface and carry heat fluxes and the liquid is thermally well-mixed within its interior. This case arises, for example, when the liquid cooled from above. The heat flux decreases as the liquid temperature decreases if the temperature of the interface is constant.

When the liquid is stagnant, F_{TL} is governed by heat conduction like F_{TS} , and is given by

$$F_{TL} = -k_l \left. \frac{\partial T}{\partial z} \right|_{z=0-} \quad (2-3b)$$

This case arises, for example, when the liquid cooled from below forms the stable stratification in density.

Let us return equation (2-1) to consider the thermal balance at the solid/liquid interface and its migration. When the position of the interface does not change, the relationship $F_{TL}=F_{TS}$ is held by the change of T_i ; T_i increases when F_{TL} becomes relatively larger and T_i decreases when F_{TL} relatively smaller. The change of T_i cannot hold the relationship $F_{TL}=F_{TS}$ when F_{TL} becomes some larger value, because T_i must be below the melting temperature of the solid. Then F_{TL} exceeds F_{TS} and hence melting of the solid proceeds with T_i fixed at the melting temperature of the solid. Similarly, the

change of T_i cannot hold the relationship $P_{TL}=P_{TS}$ when P_{TL} becomes some smaller value, because T_i must be above the melting temperature of the liquid. Then P_{TS} exceeds P_{TL} and solidification of the liquid proceeds with T_i fixed at the melting temperature of the liquid.

As discussed above, the melting temperatures of the solid and the liquid and the thermal balance at the interface determine the migration of the interface. The melting temperatures of a magma and a crust cannot be defined in a strict sense because they are multi-component material. When a multi-component material in solid state progressively melts, they can be regarded as partially molten solid with mechanical strength when the fraction of melt is low (Shaw, 1980). At this stage, the crystalline phases form an interconnected framework. However, beyond some critical melt fraction the connectedness of the crystalline framework is destroyed and the partially molten solid has been converted into partially crystallized liquid. Experimental and theoretical studies (Wickham, 1978; van der Molen and Pateron, 1979; Shaw, 1980; Marsh, 1981) indicate that there is typically a very large variation in viscosity by up to ten orders of magnitude for small changes of melt fraction and temperature in the vicinity of the critical melt fraction (50-60%). We assume that the temperature at which the critical melt fraction is attained is a sensible value to take as the effective fusion temperature (EFT) of the material in applying the theory (Huppert and Sparks, 1988b), when separation of liquid and solid phases does not occur.

EFT will vary according to the composition of the material, because it is determined by the fraction of solid and liquid phases. The EFT of the solid is generally different from that of the liquid. Therefore, we have to understand how the migration of the interface changes by the set of the EFTs of the solid and the liquid. This problem is considered in the following, when the liquid is convective or non-convective.

(1) Convective liquid

(i) When the EFT of the solid is equal to that of the liquid (Fig. 2- 2A), T_i is fixed at its EFT and the position of the interface always changes as the solid melts or the liquid solidifies. When the solid is in contact with the liquid, the finite heat flux P_{TL} expressed

in equation (2-3a) occurs simultaneously with a large (initially infinite) conductive heat flux P_{TS} in the solid. As the conductive heat flux in the solid must initially exceed any heat flux from the liquid, the formation of a chilled margin must be the first response (Fig. 2- 2Aa). As time proceeds, however, P_{TS} decreases rapidly as the conductive temperature profile relaxes. Thus there will come a time when P_{TL} exceeds P_{TS} . From then on melting at the interface occurs (Fig. 2- 2Ab). The previously solidified chilled margin will remelt, followed by the initial solid, provided that the EFT is less than the temperature of the liquid (Fig. 2- 2Ac). As T_i decreases with time, P_{TL} decreases (see equation 2-3a), there will come a time when P_{TS} exceeds P_{TL} again. The liquid begins to solidify (Fig. 2- 2Ad). When the liquid temperature becomes the EFT, convection in the liquid ceases because there is no temperature difference in the liquid. Then solidification proceeds by thermal conduction alone (Fig. 2- 2Ae).

(ii) When the EFT of the solid is lower than that of the liquid, solidification of the liquid and melting of the solid occur simultaneously. I do not consider this situation because it is unrealistic.

(iii) When the EFT of a solid is higher than that of a liquid (Fig. 2- 2B), T_i is fixed at the higher EFT when solidification or melting of the initial solid proceeds and T_i is fixed at the lower EFT when solidification or melting of the initial liquid proceeds. That is, the migration of the interface occurs like the case of the uniform EFT although T_i is different. It is noted, however, that the position of the interface does not change when T_i is between the higher and the lower EFTs. This situation will occur between (b) and (c) or (d) and (e) in Fig. 2-2A, and cannot occur in the case of the uniform EFT.

(2) Stagnant liquid

The migration of the interface position will change by the difference of the EFTs of the solid and the liquid. It is not expected, however, that the difference of the EFTs affects on the evolution of the temperature profile of the system qualitatively, because the heat transfer processes in both the solid and the liquid are conduction alone.

2.2. Numerical calculations in the one dimensional model.

According to the discussion in §2.1, it is suggested that the two phenomena, "migration of the interface" and "convection of the liquid", govern the thermal evolution of the system. Therefore, I will quantify the effects of the two phenomena using the numerical calculations on the one dimensional model of the following three cases:

Case 1: the interface migrates and the liquid convects vigorously (Fig 3b),

Case 2: the interface migrates and the liquid does not convects (Fig 3c), and

Case 3: the interface does not migrate and the liquid convects vigorously (Fig 3d).

Consider that a layer of a hot liquid with an initial thickness H_0 and temperature T_0 is in contact with a cold solid along a flat plane ($z=a$) and insulated at the other plane ($z=0$) (Fig. 2- 3a). It is assumed that the solid has a very large thickness and an initial uniform temperature T_∞ . I calculate the temperature profiles and the positions of the interface, based on the thermal balance of the equations (2-1)-(2-4). The physical parameter values and the constants used in the calculations are shown in Table 2-1. I assume that the phase change between solid and liquid occurs completely in one temperature (850 °C) and that there is no volume change associated with the phase change, because we focus upon the effects of "migration of the interface" and "convection of the liquid". In Case 3, it is assumed that the melting temperature of the solid is too high to melt and that the melting temperature of the liquid is too low to solidify.

The most important result is that the rate of the temperature decrease of the liquid is significantly large regardless of the temperature of the solid when the solid/liquid interface migrates due to melting driven by vigorous convection (Case 1). For example, when the initial liquid thickness is 1 km, the time taken the liquid temperature to become the melting temperature is about 300 years, and the time taken the liquid to solidify completely is about 10^5 years (Fig. 2- 4a). Let us see the migration of the interface in Case 1. The liquid is chilled initially but it remelts soon. Melting of the solid proceeds rapidly until the liquid temperature becomes its melting temperature. When the liquid temperature is the melting temperature, the amount of melting is almost maximum. Then,

solidification begins and proceeds slowly (Fig. 2-4b). The time at which the liquid temperature becomes the melting temperature in Case 1 is more than one order of magnitude shorter than that in Case 2 or 3. The results of the calculations in which the initial solid temperatures vary from 150 to 675 °C indicate that the effects of melting of the solid and convection of the liquid are much more important than the variation of the initial solid temperature (Fig. 2-4a).

It is noted that the rapid decrease of the liquid temperature in Case 1 is not caused by the production of a cold liquid due to melting of the solid and that it is not caused by heat loss from the liquid into the solid. The cold liquid generated by melting of the solid makes the mean temperature of the liquid decrease. The cooling processes of Case 2 and 3 and Case 1 after the liquid temperature becomes its melting temperature is governed by heat conduction in the solid. They proceed very slowly (the time scale is 10^4 -6 years when the initial liquid is 1 km thick). These facts indicate that the convection of the liquid causes the interface temperature become higher and cannot qualitatively change the rate of the heat transfer in the solid.

The model used in these calculations is not a full description of the physics of a magma system. Therefore, we should know the general laws governing the thermal history of the magma system from the results of the calculations rather than details. The important points are summarized in the following:

- (1) Heat loss of the liquid is governed by conduction in the solid. This process proceeds very slowly and is not qualitatively affected by the temperature at the interface and the convective state of the liquid.
- (2) The melting rate of the solid is determined by the heat flux from the liquid to the solid/liquid interface when the liquid is convective vigorously.
- (3) The mean temperature of the liquid decreases by the generation of the cold liquid due to melting of the solid.

It is inferred that the cooling of a magma in a crust has the two stages (Table. 2-2). One is the rapid cooling stage in which the temperature of the magma decreases rapidly when the crust melts accompanying the interface migration and the liquid convects

vigorously. The other is the slow cooling stage in which the crust does not melt or the liquid does not convect. The magma has the temperature between the initial temperature of the magma and the melting temperature of the crust in the rapid cooling stage. On the other hand, The magma has the temperature near or below the melting temperature of the crust in the slow cooling stage.

The relationships between the initial thickness of the magma and the time periods of the two stages in Case 1 are shown in Fig. 2-5. The solid line shows the time at which the difference between the liquid temperature and the melting temperature becomes 5% to the difference between the initial liquid temperature and the melting temperature. This time would be the time period of the rapid cooling stage. The dashed line shows the time at which the initial magma solidifies completely. The time difference between the solid and the dashed lines would be the time period of the slow cooling stage. The time period of the rapid cooling stage is almost proportional to the initial thickness of the magma. On the other hand, the time period of the slow cooling stage is almost proportional to the square of H_0 because the cooling is governed by thermal conduction in the solid. Thus the difference of the time periods between the rapid and the slow cooling stages increases with the initial magma thickness.

2.3. Summary of the theoretical analysis

We can understand the important factor to the thermal history of the magma system. The relationship between the temperature of a magma and the EFT of a crust is the most important. When the temperature of a magma initially exceeds the EFT of a crust, for example, when a basaltic magma is emplaced in a granitic crust, the temperature decrease of the magma and the melting of the crust would initially proceed in the rapid cooling stage until the temperature of the magma becomes the EFT of the crust. After that, the magma system will evolve in the slow cooling stage, if the EFT of the magma is higher than the EFT of the crust (Fig. 2-6a). On the other hand, when the EFT of a crust initially exceeds the temperature of a magma, for example, when a dacitic magma is emplaced in a

gabbroic crust, the magma system would evolve in the slow cooling stage and would have the magma as liquid for a long time period (Fig. 2-6a).

The results shown in Fig. 2-5 indicate that the time period of the rapid cooling stage is instantaneous, compared with that of the slow cooling stage, in the magma system with the possible length scale in the Earth. Therefore, I conclude that the EFT of the **crust** is the most important parameter to govern the property of long-lived magma in a magma system. The timing and the interval of the volcanic eruption must be considered when we discuss the genesis of the volcanic ejecta.

My results in this section indicate that when we think about the evolving magma in a crust as time proceeds, we have to consider the interaction between both the magma and the crust. The importance of the compositional effects arises for further investigations. In order to know the composition of the magma in the slow cooling stage and the liquid motion at the interface between the magma and the crust, the density change and separation of solid and liquid phases due to melting and crystallization must be understood. These problems will be investigated using the analogue laboratory experiments in the following sections.

Table 2-1. Parameter value in the calculation.

	Value	Unit
Density (ρ)	2.6×10^3 (s), 2.4×10^3 (l)	kg m^{-3}
Thermal conductivity (ks, kl)	2.4(s&l)	$\text{W m}^{-1} \text{K}^{-1}$
Specific heat	1.3×10^3 (s&l)	$\text{J kg}^{-1} \text{K}^{-1}$
Kinematic viscosity(ν)	1.0×10^2	$\text{m}^2 \text{s}^{-1}$
Latent heat of fusion(L)	2.9×10^5	J kg^{-1}
Thermal expansion coefficient(α)	5.0×10^{-5}	K^{-1}
Melting temperature (T_e)	850	K
Gravity acceleration(g)	9.8	m s^{-2}
Constant in Equation(3a) (λ)	0.1	-

(s) : the value of the solid; (l) : the value of the liquid.

Table 2-2. Properties of the rapid cooling stage and the slow cooling stage

	The rapid cooling stage	The slow cooling stage
Conditions	A crust melts and a liquid convects vigorously	A crust does not melt or a liquid is stagnant
Temperature of a magma	EFT of a crust $< T <$ The initial temperature of magma	$T \leq$ EFT of the crust

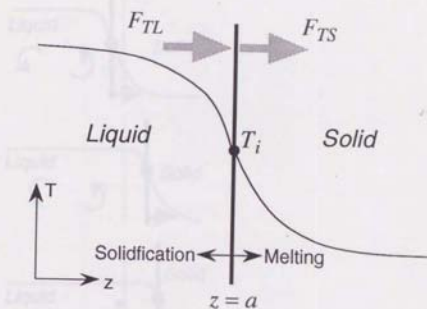


Fig. 2-1. Geometry near the solid/liquid interface. See the text.

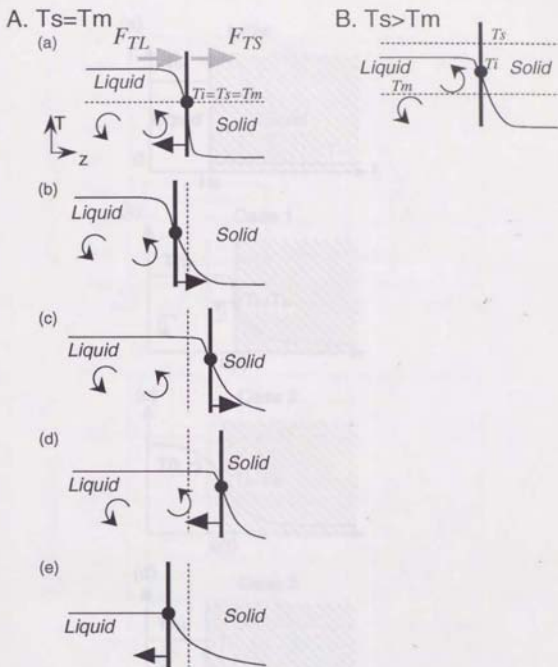


Fig. 2-2. The migration of the solid/liquid interface and the temperature profile. T_i , T_s , and T_m are the temperature at the interface, the EFT of the solid and the EFT of the liquid, respectively. A: The case in which $T_s = T_m$. Figures of (a)-(e) are arranged in order of time. B: The case in which $T_s > T_m$. The situation that the interface does not migrate can be between (b) and (c) or (d) and (e) in A.

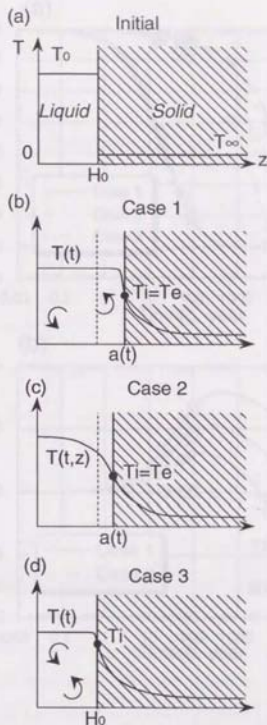


Fig. 2-3. Definition sketches for the models of §2.2. (a) The initial condition. The liquid has the temperature T_0 with the thickness H_0 . The solid has the temperature T_∞ . (b) Case 1: The interface migrates and the liquid convects. The internal temperature of the liquid is uniform because of vigorous convection. (c) Case 2: The interface migrates the liquid is stagnant. The liquid temperature is not uniform because the heat transfer process in the liquid is conduction. (d) Case 3: The interface does not migrate and the liquid convects. The internal temperature of the liquid is uniform because of vigorous convection.

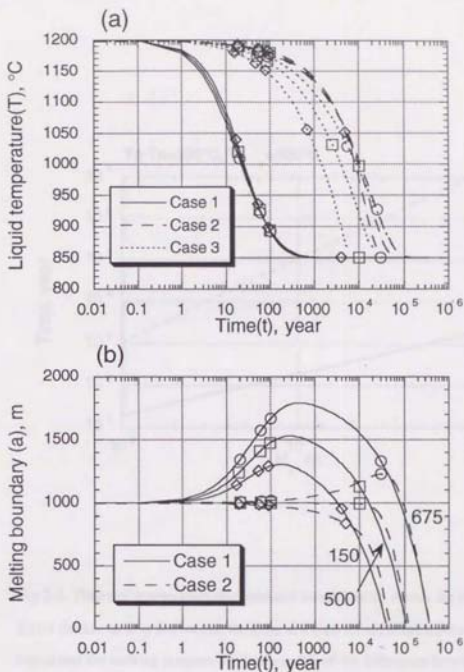


Fig.2-4. Results of the numerical calculation §2.2 in the Case 1, 2, and 3. The liquid has 1200 $^{\circ}\text{C}$ with 1 km thick initially. The numerical calculation are done in the three initial solid temperatures: circle, square and diamond are 675, 500, and 150 $^{\circ}\text{C}$, respectively. Solid, dashed, and dotted lines show the results of Case 1, 2, and 3 respectively. (a) The liquid temperature (T) versus time. In Case 2, the average temperature of the liquid is shown. (b) The position of the solid/liquid interface versus time in Case 1 and 2.

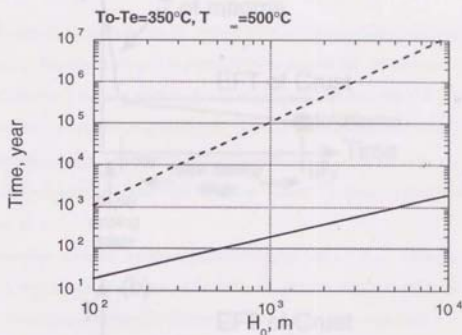


Fig 2-5. Times of temperature decrease and solidification versus the initial liquid thickness. It is shown that the time at which the difference between the liquid and the melting temperature become 5% of the difference between the initial liquid temperature and the melting temperature (solid line) and the time at which the liquid solidifies completely (dashed line).

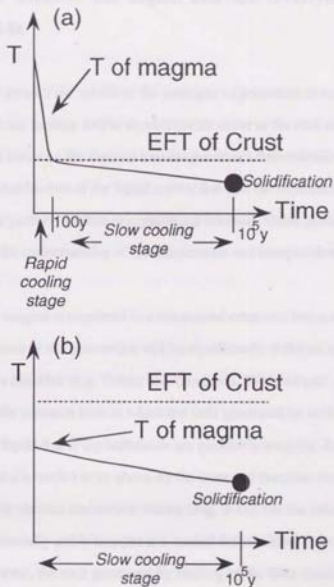


Fig.2- 6. The schematic diagram showing the change of the temperature of the magma with time. (a) The case in which the EFT of the crust < the initial temperature of the magma. (b) The case in which the EFT of the crust > the initial temperature of the magma.

3. Analogue Experiments. Part 1 : Melting and Crystallization at the Interfaces between the Liquid and the Overlying and/or Underlying Solids

In this section, I present the results of the analogue experiments to consider the condition under which the melting and/or crystallization occur at the roof and the floor of the magma chamber. I focus on the thermal transfer processes theoretically in § 2, but does not consider the mechanism of the liquid convection and the separation of the liquid and solid phases in the partially molten or crystallized material. These processes are important to improve the understanding of the temperature and compositional profiles in the magma system.

When a basaltic magma is emplaced in a continental crust and forms a magma chamber, the mechanisms of the convection will be significantly different at the roof and the floor in the magma chamber (e.g. Turner and Campbell, 1986; Jaupart and Tait, 1995). Consider the common case in which the melt generated by melting of the crust and the residual liquid due to crystallization are positively buoyant. At the roof of the chamber, the magma is cooled from above by the crust and becomes thermally unstable. Therefore, the thermal convection occurs (Fig. 3-1a). On the other hand, at the floor, the magma is thermally stable because it is cooled from below. Thus the magma is thermally stable. However, the melt generated by melting of the floor crust and the residual liquid released by the crystallization near the cold floor are positively buoyant because of their compositional effects. Therefore, the compositional convection occurs (Fig. 3-1b).

When these different mechanisms of convection and their interaction occur in the magma system, they will give large effects on the heat transfer and the temperature and compositional profiles of the system. I discuss the effects of the processes caused at the roof and the floor of the magma chamber on the thermal and compositional evolution of the magma system, based on the results of the experiments using a hot liquid and a cold solid in the binary eutectic system.

3.1. Experimental technique and conditions

The system used in the experiments

Natural magmas and crusts are multi-component materials and have complicated phase relations in crystallization and melting. The important properties of multi-component materials are (i) the change of its density due to both temperature and composition and (ii) the coexistence of solid and liquid phases between the solidus and the liquidus. The essence of the physics may be illustrated with a binary eutectic system. The experiments were carried out using the simple binary eutectic system, $\text{NH}_4\text{Cl-H}_2\text{O}$ (Fig.3-2). The physical parameter values are shown in Table 3-1.

The solid used in the experiments initially had the eutectic composition and the temperature slightly below the eutectic temperature (19.7wt%, about -16°C). The liquid was saturated 28wt% NH_4Cl aqueous solution (23.5°C) (Fig.3-2). It is considered that this system simulates the set of a basaltic magma and a granitic crust in the following two points. (i) Crystallization of the liquid releases the light, cold liquid and (ii) melting of the solid generates the light, cold liquid.

I will present the results of the three experiments in this section. The three experiments are called the roof experiment, the floor experiment and the both sides experiment (Fig.3-3, Table.3-2). The roof experiment is that the liquid was in contact with the solid at the top of the liquid. The floor experiment is that the liquid was in contact with the solid at the bottom of the liquid. The both sides experiment is that the liquid was in contact with the solid at both the top and the bottom of the liquid. The roof and the floor experiments have been carried out to understand the processes caused at each interface. The both sides experiment has been carried out to understand the interaction between the processes at the roof and the floor. Only the geometry of the solid and the liquid was different while other conditions were almost the same in this series of the experiments.

Apparatus

Experiments were carried out in a Perspex tank with inner dimensions of 10 x 10 x 30 cm high and 1 cm wall thick (Fig.3-4). The side hole of the tank and an irrigator were connected with a silicone tube to adjust the level of the liquid in the roof and the both sides experiment. All sides were thermally insulated from the laboratory with foam plastic with 5 cm thick. The form plastic was removed periodically for a short time when visual observations of the interface positions and the liquid motion were made. Flow visualizations were made with the shadowgraph technique.

The temperatures were monitored using Alumel-Chromel (K type) thermocouples. The maximum number of the thermocouples used in the experiments was 30. The junction of each thermocouple coated with epoxy and was put near the center of the experimental tank at fixed height at 1 cm vertical intervals. The wire of each thermocouple was routed horizontally to the wall of the tank through the glass tube with 2.5 mm diameter, and then vertically along the wall up to the top of the tank, because I want to make the effect of the thermocouples on the vertical temperature profile as little as possible.

Procedure

The first step in each experiment was the preparation of a solid mixture of NH_4Cl and ice with the thermocouple array by cooling an NH_4Cl solution of the eutectic composition strongly. In the roof experiment, the solid was made in another tank with the same horizontal size as the experimental tank. The eutectic NH_4Cl solution was cooled in the tank and removed from the tank as solid mixture after it solidified completely. The solid was suspended in the experimental tank. The tank was then filled with 28 wt% NH_4Cl solution until the level of the bottom of the solid and the run started. The level of the liquid was adjusted by the irrigator during the run. In the floor experiment, the solid was made at the bottom of the experimental tank. After the eutectic solution solidified completely, 28 wt% NH_4Cl solution was poured into the tank until the objective level, and then the run started. In the both sides experiment, the roof and the floor solids were

made in the same ways as the roof and the floor experiments, respectively. The liquid was poured into the experimental tank until the objective level and was in contact with the roof solid suspended. Then the run started. The liquid is dyed in red to observe mixing between the original liquid and the melt generated by melting of the solid.

During the experiments, the visual observations were made in every 5 minutes from the start of the run to 30 min, every 10 minutes from 30 to 60 min, every 20 minutes from 60 to 120 min, and then every 30 minutes. I observed the flow motion of the liquid, the layer structure of the system, and the interface position of regions formed in the experimental system.

The temperatures were sampled in every 3 seconds from the start to 30 min, every 12 seconds from 30 to 90 min, and then every 60 seconds throughout each run.

Samples of liquid were periodically withdrawn from the tank at several heights (typically 4 heights at 3 cm vertical intervals) every 10 minutes from the start to 60 min, every 20 minutes from 60 to 120 min, and then every 30 minutes throughout each run. The refractive index of the liquid sample measured allowed deduction of the concentration of solute to ± 0.2 wt%.

3.2. The roof experiment

Evolution of convection, crystallization and melting

I now give a description of the roof experiment. The three layers were formed below the roof solid in this experiment. They are the upper liquid layer, the lower liquid layer and the sediment layer.

As soon as the experiment started, heat flux from the liquid to the interface occurred and melting of the roof solid and crystallization of the original liquid began to proceed simultaneously (Fig.3-5) (Plate.3-1). The melt of the roof solid had the eutectic composition and was less NH_4Cl content than that of the underlying original liquid. Since the density of the NH_4Cl aqueous solution depends more strongly upon the

composition than the temperature, the melt of the roof solid formed a stable separate layer (the upper liquid layer) of the eutectic composition between the roof solid and the underlying liquid despite the fact that it was colder. The upper liquid layer was colorless through the run and the interface between the upper and the lower liquid layers were easy to follow visually (Plate.3-3). This fact indicates that the dyed original liquid was not mixed into the upper liquid layer. The interface between the upper liquid layer and the roof solid (the solid front) migrated upward due to melting of the roof solid and the thickness of the upper liquid layer increased with time (Fig.3-6). The convective motion was already observed in the upper liquid layer at 10 min and then was maintained through the run. The interface between the upper and the lower liquid layer was very sharp and almost at the constant position.

The original liquid which was initially saturated in NH_4Cl formed the lower liquid layer (Fig.3-5). The convection in the lower liquid layer was observed through the run (Plate.3-2). I did not observe that there was no convective flow through the interface between the upper and the lower liquid layers. At 40 min, the weak dyed layer with about 1 cm thick could be observed just below the interface between the upper and the lower liquid layers. This layer might form by a little mixing of the upper and the lower liquid layers. Crystallization of NH_4Cl crystals proceeded in the lower liquid layer cooled from above. Most of NH_4Cl crystals settled at the bottom of tank and formed the sediment layer. A part of the crystal moved with the convective liquid in the lower liquid layer. The thickness of the lower liquid layer decreased with time because the interface between the upper and the lower liquid layers did not migrate while the thickness of the sediment layer increased with time (Fig.3-6).

The sediment layer consisted of the settled NH_4Cl crystals from the lower liquid layer and the interstitial solution. The upward flow from the surface of the sediment layer was not observed.

Evolution of temperature and compositional profiles

The upper liquid layer has the eutectic composition and higher temperature than the eutectic temperature. The thermocouple at 13 cm high above the bottom of the tank (almost 1 cm high above the interface between the upper and the lower liquid layers) entered the upper liquid layer at 20 min and indicated that the temperature increased at that height (Fig.3-7a). At 25 min, the temperature at that height began to vibrate and decreased to about -10 °C rapidly (Fig.3-7a). The interpretation of this change of the temperature at 13 cm high is that when the temperature vibration occurred, the weak convection became more vigorous. The Rayleigh number of the upper liquid layer is expressed as

$$R_a = \frac{\alpha g \Delta T H^3}{\kappa \nu} \quad (3-1)$$

where α , g , ΔT , H , κ and ν are thermal expansion coefficient, gravity acceleration, the difference between temperatures at the solid front and the interface between the upper and the lower liquid layers, thickness of the upper liquid layer, thermal diffusivity and kinematic viscosity, respectively. The Prandtl number ($= \nu/\kappa$) of the liquid in this experimental system is 5.8 and hence the Rayleigh number in which the transition to turbulent convection occurs is about 10^5 (Kurishnamurti, 1970b) (Fig.3-9). The estimated Rayleigh number of the upper liquid layer increased with time and exceeded 10^5 at 20 to 25 min. The result of the experiment is consistent with the theory of fluid mechanics. After the thermocouple at 14 cm high above the bottom of the tank entered the upper liquid layer at about 40 min, the temperatures at 13 and 14 cm high above the bottom of the tank were almost equal (Fig.3-9a, Fig.3-10). This fact indicates that the upper liquid layer was well-mixed thermally at this time.

The lower liquid layer has almost uniform temperature (Fig.3-10). The Rayleigh number of the lower liquid layer was large enough to convects turbulently (Fig.3-8). The temperature of the lower liquid layer was always equal to the liquidus temperature (Fig.3-10) and decreased with time.

The sediment layer had the profile of the temperature that increase downward (Fig 3-10). The change of the temperatures at the fixed position in the lowest part of the system is shown in Fig.3-7c. The temperature decreased when the thermocouples were in

the lower liquid layer but increased temporally when they entered the sediment layer (Fig.3-7c).

Melting rate and heat transfer process

The heat transfer is discussed based on the melting rate of the roof solid. The change of the melting thickness of the roof solid is shown in Fig.3-11. The melting thickness of the roof solid increased rapidly between 20 min and 25 min. This fact indicates that the heat flux from the upper liquid layer to the solid front increased by the transition to turbulent convection in the upper liquid layer. This is consistent with the consideration on the Rayleigh number discussed above.

I estimate the heat flux from the upper liquid layer to the solid front from 25 min to 100 min. This heat flux determines the melting rate of the roof solid. In the experiment, the temperature of the roof solid was near the eutectic temperature. Thus, the heat loss into the roof solid was negligible. Then the heat flux F_T is expressed as

$$F_T = \rho L \frac{da}{dt} \quad (3-2)$$

where ρ , L and a are the density of the roof solid, latent heat of fusion of the roof solid and the position of the solid front. Therefore, F_T can be estimated from the migration rate of the solid front. The relationships between F_T and the difference (ΔT) between the temperature of the upper liquid layer and the temperature of the solid front (= the eutectic temperature) are shown in Fig.3-12. F_T is roughly proportional to $\Delta T^{4/3}$. I conclude that when the Rayleigh number is large, the heat flux to the solid front is determined by vigorous thermal convection of the upper liquid layer, which can be expressed by equation (2-3a).

The melting thickness of the roof solid is compared with the prediction of the physical model (Fig.3-11). The melting thickness of the experiment is much larger than the prediction of the model in which heat conduction is only the heat transfer process after 20 min. The melting rate of the experiment is smaller than the model of Huppert and Sparks (1988a,b) in which it is assumed that both the upper and the lower liquid layers are convective turbulently from the initial state (Fig.3-11a). The melting rate in the

experiment is also smaller than the model in which it is assumed that the upper liquid layer is stagnant until 20 min and then becomes convective vigorously (solid line 1 in Fig.3-11b). I cannot fully understand what causes the result of the experiments to differ from these models. One possible reason is that the lower liquid layer was divided into several layers. The formation of the weak dyed layer in the lower liquid layer was observed in the experiments. Solid lines 2 and 3 in Fig.3-11b are the prediction of the model in which the lower liquid layer is divided into 2 and 3 convective layers with the same thickness, respectively. As the number of layers increases in a given thickness, the temperature step between each layer decrease and hence the heat flux to each interface decrease.

Summary

The important results of the roof experiment are summarized in the following:

- (1) The melt generated by melting of the roof solid forms a separate layer between the roof solid and the underlying original liquid. Mixing of this separate layer and the underlying original liquid is negligible.
- (2) The heat flux from the upper liquid to the solid front layer is determined by the thermal convection of the upper liquid layer.

3.3. The floor experiment

Evolution of convection, crystallization and melting

The characteristic of the floor experiment is the formation of two layers: one is the mushy layer where NH_4Cl crystals and interstitial aqueous solution coexist just above the floor solid due to crystallization from the liquid and the other is the liquid layer (Fig.3-13).

As soon as the experiment started, the solid/liquid interface (the solid front) migrated downward monotonically by melting of the floor solid (Fig.3-14a, Plate.3-4,

5). Simultaneously, the mush formed by crystallization cooled from below (Fig.3-14b). Crystallization of the system occurred in the mush and at the mush/liquid interface (the mush front), but did not occur in the liquid above the mush front. The mush front grew upward very rapidly in early 5 min. Then the mush front migrated upward more slowly, and then began to migrate downward after about 80 min. The downward migration of the mush front from 80 to 170 min occurred by falling down of the whole mush with the solid front that migrates downward by melting of the floor solid. The mush thickness increased with time during this stage. Then the mush thickness began to decrease at 170 min. At this time, the crystals at the mush front remelted. This fact indicates that crystallization and remelting occurred.

The convection began as soon as the experiment started and it continued through the run. The cold, light liquid generated by melting of the floor solid and the light liquid released by crystallization in the mush rose up as plume and mixed with the liquid above the mush layer. This convection was the *compositional convection* caused by the compositional change of the liquid. In the early stage, the many plumes violently rose up. Gradually, the plume motions became weaker. I could see the two types of the plumes at 30 min: one was the narrow plume that disappeared at the middle height of the liquid and the other was the thick one that reached up to the top of the liquid. The narrow plumes gradually became weaker and then could not be observed at about 80 min. On the other hand, the thick plumes could be observed through the run (Plate.3-6).

These two types of plumes have been reported in the previous experimental studies about crystallization of the liquid cooled from below (e.g. Chen et al.,1993; Tait and Jaupart, 1989,1992). They reported that the compositional convection began by the onset of the narrow plumes, followed by the onset of the thick plumes. It has been observed that the narrow plumes rise up near the mush front while the thick plume rises up from within the mush. Worster (1992) have been theoretically analyzed the linear stability in the mush and found the independent two modes of the instability: one occurs near the mush front and the other occurs within the mush. The former corresponds to the narrow plume and the latter to the thick plume. In my experiment, thick plumes existed in

the early stage of the experiment. This fact suggests that melting of the floor solid enhances the onset of the thick plume, compared with the results of the crystallization experiments.

I could observe vertical conduits without crystals in the mush and holes of the tops of the conduits on the surface of the mush front in the experiment. The conduits penetrated to the bottom of the mush. The thick plumes rose up from the holes on the surface of the mush front. They have been called "chimneys" (e.g. Tait and Jaupart, 1992). The number of the chimney increased rapidly in the early stage of the experiment and reached a maximum. After that, the number of the chimneys began to decrease while diameter of each hole increased with time.

Evolution of temperature and compositional profile

I present the change of the temperature profile of the experimental system (Fig.3-15). The temperature in the mush increased upward through the run, and the temperature gradient in the mush was larger than that in the liquid. The temperature in the liquid was almost uniform and decreased with time from the start of the run to 20 min. From 20 to 80 min, the temperature gradient at the lower part of the liquid was observed and the temperature at the upper part of the liquid became lower than below by about 2 °C (25-60 min in Fig.3-15). This fact suggests that the cold, light compositional plumes from the solid front and the mush reached to the upper part of the liquid before they heated up to the surrounding temperature and ponded there. From 80 min to the end of the run, the temperature of the liquid increased upward, reached a maximum at the middle part of the liquid, decreased upward, and increased upward again.

NH_4Cl content of the liquid above the mush decreased with time because it was continuously mixed with the compositional plumes with low NH_4Cl content which consisted of the melt generated by melting of the floor solid and the interstitial liquid in the mush (Fig.3-16a,b). All NH_4Cl contents of the liquid at the fixed heights and at the mush front decreased with time (Fig.3-16a). The liquid had the compositional profile that

the NH_4Cl content decreased upward. The difference between the NH_4Cl contents at the mush front and the uppermost part of the liquid increased with time (Fig.3-16b).

Now let us see the relationship between the temperature profile and the liquidus profile estimated by the compositions in the liquid (Fig.3-16). The liquidus decreased upward, corresponding to the upward decrease of NH_4Cl content of the liquid. From the start of the run to 60 min, the temperature at the mush front was lower than the liquidus there while the temperature at the upper part of the liquid was higher than its liquidus. The liquid near above the mush front was supercooled because this stage was before the crystal-liquid interface reached thermodynamic equilibrium. After 80 min, the temperature at the mush front was almost equal to the liquidus there, and all liquid above the mush front had higher temperature than its liquidus.

The temperature at the mush front is equal to the liquidus of the liquid composition there. The position of the mush front is determined by both temperature and liquid compositional profiles changing with time. The migration of the mush front can be explained in the following (Fig.3-16). I could assume the thermodynamic equilibrium in the mush and at the mush front; the interstitial liquid in the mush and the liquid at the mush front have the liquidus temperature. The temperature and the liquidus corresponding to the composition at the mush front decreased with time. If the decrease of the temperature at the mush front is more than the decrease of the liquidus due to the decrease of the NH_4Cl content of the liquid there, the highest point of liquidus migrates upward and hence the mush front migrates upward. On the other hand, if the decrease of the liquidus due to the change of the NH_4Cl content of the liquid at the mush front is more than the decrease of the temperature there, then the highest point of liquidus migrates downward and the mush front migrates downward.

Melting rate and heat flux

The migration of the solid front is determined by the heat flux from the mush to the solid front. The migration of the solid front in the floor experiment is shown in Fig.3-18, compared with the predictions of two physical models: one is the turbulent convection

model in which it is assumed in the turbulent convection model that the region above the solid front is thermally well-mixed by the compositional convection and hence has the uniform temperature, and the other is the diffusion model in which it is assumed that the liquid is not convect and the heat transfer process in the system is only the thermal conduction. It can be seen that the migration of the solid front in the experimental result was much smaller than that in the turbulent convection model while is close to that in the diffusion model, although the compositional convection could be observed in the experiments. This fact indicates that the temperature gradient just above the solid front was close to that in the diffusion model in the experiment and suggests that the mush and the liquid which were convective were not thermally well-mixed effectively by the compositional convection. It is suggested, in other words, that the compositional convection carry a low heat flux.

The phenomena that the compositional convection carries a low heat flux can be seen commonly in double-diffusive convection when the diffusion coefficient of the composition causing convective instability is smaller than the diffusion coefficient of the heat making the system stable in density. Many further studies report these phenomena (e.g. Chen and Turner, 1980; Tait and Jaupart, 1989,1992; Chen and Chen, 1991; Jaupart and Tait, 1995).

In order to understand this phenomenon, let us consider how convection carries a heat. Generally, the temperature of the upwelling flow is different from that of the downwelling flow in a convective system. Convective heat flux occurs by this temperature difference. When the convective instability due to cooling from above occurs, the temperatures of the downwelling plumes must be lower than those of the upwelling plumes. Therefore, this convective plumes carry the heat flux necessarily. On the other hand, consider that the convective instability occurs by the compositional difference. If the cold, light upwelling plumes are heated up by the hot, dense surrounding liquid and become the same temperature as the surrounding liquid, the upwelling plumes become lighter and the convective instability becomes larger. That is, the convection is maintained although it does not carry the heat flux.

When the composition that makes unstable density gradient has much smaller diffusion coefficient than heat that makes stable density gradient, as occurring in this experiment, the convection due to upwelling of finger-like plumes with low solutal content and low temperature occurs and the plumes carry the vertical heat flux (Turner, 1979). The heat flux carried by the plumes depends on upwelling velocity, spacing and figure (especially diameter) of the plumes because it is determined by the heat exchange between the plumes and the surrounding mush or liquid. Thus when the upwelling velocity and the diameter of the plume are small, the plumes cannot carry the heat flux effectively because the horizontal temperature difference becomes small, and vice versa.

The temperature of plumes at the mush front was only a little lower ($1\sim 2\text{ }^{\circ}\text{C}$) than the surrounding temperature in this experiment. This temperature difference is much smaller than the temperature difference between the solid front and the horizontally averaged temperature at the mush front. This result indicates that the horizontal temperature gradient induced by the upwelling cold plumes in the mush relaxed rapidly and that the plumes did not carry the vertical heat flux effectively.

The temperature gradient at the solid front resembles those that would be predicted by the diffusion model in the experiment, whereas the liquid decreased in temperature with time, the profile of which was relatively uniform. This profile is clearly different from that the diffusion model (Fig.3-19). Additionally, the temperature at the upper part of the liquid was a little lower than below. This indicates that the compositional convection can somewhat carry the heat flux in the liquid region.

Summary

The important results of the floor experiment are summarized in the following:

- (1) The convective plumes of the melt generated by the floor solid and the interstitial liquid in the mush mix with the overlying liquid, the composition of which changes with time.
- (2) Compositional convection cannot effectively carry a heat flux.

3.4. The both sides experiment

Evolution of convection, crystallization and melting

In this experiment, melting at both the roof and floor solids and the formation of the mush above the floor solid could be observed simultaneously as soon as the experiment started (Plate.3-7).

The system had the two liquid layers from the start of the run to 40 min : one is the upper liquid layer of the melt generated by the roof solid and the other is the lower liquid layer of the original liquid mixing with the compositional plume from the floor (Fig.3-20b). The interface between the lower and the upper liquid layers did not almost migrate during this stage. As soon as the experiment started, the vigorous convection due to the downwelling cold plume and the upwelling compositional plume in the lower liquid layer could be observed (Plate.3-8). The thermal convection in the upper liquid layer could be observed at 20 min. The mush above the floor solid grew by crystallization cooled from below and by sedimentation of the crystals from the lower liquid layer cooled from above (Fig.3-21).

From 40 min, the lower liquid layer was divided into several convective layer layers (Fig.3-20c). Their thicknesses were typically 1~2 cm (Plate.3-9). The maximum number of these layers is eight at about 90 min. The temperatures of these layers decreased upward (Fig.3-24).

The phenomenon that a liquid is divided into convective several layers is commonly observed when a convective liquid has several components that cause the density of the liquid to change (double-diffusive convection). When one component with smaller diffusivity becomes stable and another component with larger diffusivity becomes unstable in liquid density, the liquid layer was divided into several layers and each layer was convective and exchanges the heat and the composition through the interface of the layers by only diffusion process (e.g. Turner, 1979). In this both sides experiment, the formation of the several convective layers in the lower liquid layer resulted from the following two effects. (1) The compositional convection caused by melting of the floor

solid and crystallization in the mush made the compositional gradient on which the NH_4Cl content decreased upwards. In the floor experiment, I could observe the compositional gradient in which the NH_4Cl content decreased upwards. In other words, the compositional convection made the liquid be stable in density on composition, which has much smaller diffusivity than heat. (2) Cooling from above made the temperature gradient on which the temperature in the liquid decreased upwards. That is, the liquid became thermally unstable. The temperature and compositional gradients by these two effects would cause the lower liquid layer to divide into several convective layers, which are called double-diffusive layers here after.

The interface between the upper and the lower liquid layers was very sharp and the upper liquid layer was colorless by 80 min. After 80 min, the interface migrated downward and the upper liquid layer gradually dyed (Fig.3-20d, Fig.3-21, Plate.3-9). This fact indicated that overturning between the upper and the lower liquid layers proceeded. The double-diffusive layers in the lower liquid layers were eroded one by one from above by the upper liquid layer. The interface continuously migrated downward and reached the mush front at 250 min (Plate.3-11). In addition, I could observe the new interface near the upper solid front at 160 min (Plate.3-10). The interface between this new layer and the upper liquid layer also migrated downward with eroding the upper liquid layer.

Evolution of temperature and compositional profiles

The temperature change with time was complicated because the thickness and the number of the layers formed in the upper and lower liquid layers changed.

I present the change of the temperatures measured at the fixed points in Fig.3-22. The position of the 13.2 cm was in the roof solid initially. After the thermocouple at 13.2 cm high entered the upper liquid layer, the temperature of it increased by 50 min. Then it fluctuated violently and began to decrease at about 50 min. It would be because the convection became turbulent as the same phenomena were observed in the roof experiment.

The temperature at 13.2 cm high slightly decreased from 50 to 70 min because the temperature of the upper liquid layer was cooled from above (Fig.3-22a). Then the temperature at 13.2 cm high increased continuously from 70 to 150 min (Fig.3-22a). The time when the temperature began to increase was the time when the interface between the upper and the lower liquid layers began to migrate downward. The increase of the temperature resulted from the continuous mixing of the cold liquid in the upper liquid layer with the warmer liquid in the lower liquid layer. The temperatures at 12, 11, 10 cm high also began to increase at 75, 11, 130 min, respectively (Fig.3-22b). These times corresponded to the times when the interface between the upper and the lower liquid layers passed those positions.

At 150 min, the temperature of 13.2 cm high suddenly dropped. Then the temperature of 12 cm high also dropped up to the same temperature as 13.2 cm high at 170 min, followed by the temperatures at 11, 10 and 8 cm high at 200, 215, and 240 min, respectively. The time when the sudden drop of the temperature at each position occurred was equal to the time when the interface between the new liquid layer (Fig.3-20e). The new liquid layer produced by melting of the roof solid was colder than the liquid below it, so that the temperature suddenly dropped when the thermocouple at each position entered the new liquid layer. On the other hand, the temperature of each position after the sudden drop in temperature gradually increased. This was because the temperature of the new liquid layer continuously increased by mixing with the underlying warmer liquid.

The temperatures in the mush did not fluctuate largely (Fig.3-21c). The thermocouples at 1 and 2 cm high were in the original liquid layer at the start of the run and entered the mush at 4 and 30 min, respectively. The temperatures at these two positions monotonically decreased. The thermocouples at 0 and -2 cm high were at the initial solid interface and in the floor solid at the start of the run, respectively. The temperatures at these two positions did not change monotonically.

The composition of the lower liquid layer decreased with time (Fig.3-22a). The compositions at 4 heights in the lower liquid layer were almost equal to the liquidus

compositions estimated by the temperature at their heights from the start of the run to 60 min (Fig.3-24). After 80 min, the NH_4Cl contents of the lower liquid layer became less than the NH_4Cl contents of the liquidus estimated by the temperatures, and, in other words, the liquid became undersaturated (Fig.3-24). The NH_4Cl content in the lower liquid layer decreased upward like the results of the floor experiment. Thus the compositional convection makes the body of the overlying liquid less NH_4Cl and makes the compositional profile that the NH_4Cl content decreases upward in the overlying liquid.

Formation of double diffusive layers and its stability

The result of the floor experiment indicated that compositional convection made the compositional gradient in the liquid layer above the mush, in which the NH_4Cl content of the liquid decreased upward. The liquid above the mush became superheated because the compositional plumes from the solid front and the interior of the mush were heated up in the mush by the liquid and the crystals around the plumes until the plumes reach the mush front and mixed with the liquid. In the floor experiment, the upper surface of the liquid was insulated thermally and hence the temperature in the liquid increased upward. Therefore, the liquid was stable thermally and compositionally (Fig.3-15).

In the both sides experiment, however, the liquid was also cooled by the roof solid. The liquid with less NH_4Cl content in the upper part of the lower liquid layer due to mixing with the superheated compositional plume was cooled by cooling from above so that it became colder. The cold liquid of the upper part in the lower liquid layer became unstable in density and fell down as downwelling plumes. These cold plumes were less concentrated while the temperature and NH_4Cl content of the liquid around the plumes increased downward. Since the diffusivity of heat is much larger than that of chemical species, the plumes would increase in temperature rather than in NH_4Cl content. Therefore, the densities of the plumes would decrease by increase of their temperature and could become equal to the liquid density around them before the plumes reach the bottom of the lower liquid layer, so that the plume could not fall any more. The plumes

were heated up by the surrounding liquid because the liquid temperature increased downward. They again decreased in density and would turn into the upward plume. These processes would cause the lower liquid layer to divide into several double diffusive layers.

In the both sides experiment, I observed that the upper liquid layer mixed with the lower liquid layer by overturning. This phenomenon could not be observed in the roof experiment. Let us consider why phenomena occurred. This reason will be illustrated by Fig.3-25. The lower liquid layer is on the liquidus at t_1 . The upper liquid layer is heated up by the lower liquid layer and has the temperature above its liquidus. Then the upper liquid layer decreases in temperature as the lower liquid layer loses its heat by the upward and downward heat flux and hence becomes cold. Thus the density of the upper liquid layer increases with time (t_1 to t_3). On the other hand, the temperature and compositional path of the lower liquid layer is determined by two effects: one is cooling of the lower liquid layer by heat loss and the other is mixing with the compositional plumes superheated. The former effect makes the liquid keep on its liquidus but the latter one makes the liquid superheated. When the latter dominates the former, the liquid can become superheated as time proceeded (t_2 , t_3). The upper and the lower liquid layers are stable in density at t_2 in Fig.3-25. If the temperatures and the compositions of the upper and the lower liquid layers reach the set which is illustrated at t_3 in Fig.3-25, the density of the upper liquid layer exceeds that of the lower liquid layer and the overturning between the upper and the lower liquid layers begins.

It was observed in the both sides experiment that the temperature of the upper liquid layer decreased from 50 to 70 min and the temperature of the lower liquid layer became above its liquidus by continuous mixing with the compositional plumes after 60 min.

The formation of the double-diffusive layers and the overturning between the upper and the lower liquid layers are very attractive phenomenon when the geological implications are considered based on the experimental results. These phenomena are governed by the delicate balances of the temperature and compositional changes. In this

experiments, however, the heat flow from the outside of the experimental system was not quantified. Thus I cannot discuss the number of the double-diffusive layers and the time of the onset of the overturning, which are important to heat transfer and chemical evolution of the system.

Summary

The important results of the both sides experiment are summarized in the following;

- (1) The thermal convection due to cooling at the roof solid and the compositional convection due to melting and crystallization at the floor solid simultaneously occur.
- (2) The upper liquid layer which is separated chemically, the lower liquid layer which is mixing with the compositional plumes, and the mush form in the early stage of the experiment.
- (3) The compositional convection makes the stable compositional gradient in the liquid and the cooling from above makes the unstable temperature gradient in the liquid above the mush front. These temperature and compositional gradients enhances the formation of the double-diffusive layers in the liquid.

3.5. Comparisons of the results of three experiments

The phenomena in the both sides experiment are approximately the superposition of the phenomena in the roof and floor experiments in the following three points. (1) Cooling of the liquid caused the thermal convection. (2) Melting and crystallization at and near above the floor solid caused the compositional convection. (3) The formations of the upper and the lower liquid layers and the mush occurred.

The interaction effects of the roof and the floor processes in the both sides experiment, however, make the temperature and compositional profiles and the heat fluxes to the roof and the floor solids different from those in the roof or the floor experiments. The interaction effects on the heat flux to the roof and the floor solids are discussed from view point of melting rate of the solid.

According to the results of each experiment, total melting thickness of the both sides experiment is more than that of the roof or of the floor experiments (Fig.3-25a). The melting thickness of the floor solid in the both sides experiment is as much as that in the floor experiment (Fig.3-26c). On the other hand, melting thickness of the roof solid in the both sides experiment is less than the roof experiment (Fig.3-26b). The similarity of melting of the floor solid in the both sides and the floor experiments can be explained in the following: the compositional convection cannot effectively carry a heat flux in these experiments and the thermal convection gives no effect on the temperature profile in the mush layer in the both sides experiment. The temperature change in the liquid layer above the mush affects melting of the floor solid by thermal conduction in the mush layer. This process proceeds very slowly so that cannot change the heat flux at the mush/solid interface during the duration of the experiment. On the other hand, Melting of the roof solid in the both sides experiment is governed by the convective heat flux like the roof experiment. Its heat flux is determined by the temperature difference between the temperatures in the liquid and at the interface. Therefore, melting rate of the roof solid decreases when the liquid temperature is relatively low (Fig.3-27). The temperature of the upper liquid layer in the both sides experiment was lower than that in the roof experiment because the lower liquid layer in the both side experiment had lower temperature by cooling from above and below and hence the heat flux from the lower liquid layer to the interface between the upper and the lower liquid layers. Mentioned above, the compositional gradient generated by compositional convection enhances the formation of double diffusive layers. Thus we can see that the compositional convection gives indirect effect on the heat flux to the solid/liquid interface at the roof solid.

3.6. Summary of the experimental results

I summarize the characters of the thermal and material transport in the solid-liquid system, based on the results of the roof, the floor and the both sides experiments, in the following:

(1) The liquid generated by melting of the roof solid forms a separate layer with negligible mixing with the underlying liquid. On the other hand, the liquid generated by melting of the floor solid mixes with the overlying liquid, which changes in composition with time.

(2) The solid/liquid interface at the top of the liquid causes the liquid to convect thermally, while at the floor a liquid to convect compositionally. This difference profoundly changes the mechanisms of the heat transfer. In compositional convection, unstable plume becomes more buoyancy by the uniformization of the horizontal temperature. Therefore, convective motion is maintained not to carry heat flux. On the other hand, in thermal convection, the temperature difference between upwelling and downwelling flows causes the liquid to convect. When the temperature of upwelling flow is equal to that of downwelling flow, thermal convection ceases. That is why melting of the solid/liquid interface at the roof is governed by the convective heat flux and at the floor do not have the difference from the thermal conduction model.

(3) The compositional convection cannot effectively carry heat flux and hence give less effect on the temperature decreasing of the liquid. However, it causes the formation of the compositional gradient in the lower liquid layer. This compositional gradient enhances the formation of double-diffusive layers and decreases the heat flux to the roof. Thus the compositional convection indirectly gives the effect on the heat flux of the system.

Table 3-1. Parameter values of the experimental system. Values for the laboratory experiment with an aqueous NH_4Cl solution. The data have been collected from a variety of sources including International critical table (1929), Chronological Scientific Tables (1995), Handbook of Chemistry (1984), and CRC Handbook (1975) and Bennon and Incropera (1986b).

	NH_4Cl solid	H_2O solid	Aqueous solution	Unit
Density	1.52×10^3	0.971×10^3	See below	kg m^{-3}
Specific heat	1.60×10^3	1.77×10^3	3.36×10^3	$\text{J kg}^{-1} \text{K}^{-1}$
Thermal conductivity	2.5	2.2	0.62	$\text{W m}^{-1} \text{K}^{-1}$
Latent heat of dissolution	2.2×10^5	3.34×10^5	-	J kg^{-1}
Viscosity	-	-	1.3×10^{-3}	Pa s
Solutal diffusion coefficient	-	-	2.0×10^{-9}	$\text{m}^2 \text{s}^{-1}$
Thermal expansion coefficient	-	-	3.83×10^{-4}	K^{-1}
Solutal expansion coefficient	-	-	0.257	-
Eutectic temperature	-	-	-15.4	$^{\circ}\text{C}$
Eutectic composition	-	-	19.7	wt%

Density of aqueous solution

$$\rho = (1.000 + a_1 T + a_2 T^2 + a_3 C + a_4 C T + a_5 C T^2 + a_6 C^2 + a_7 C T^2 + a_8 C^2 T^2) \times 10^3$$

$$a_1 = -1.021 \times 10^{-4}, a_2 = -3.320 \times 10^{-6}, a_3 = 3.430 \times 10^{-3}, a_4 = -1.854 \times 10^{-5},$$

$$a_5 = 1.840 \times 10^{-7}, a_6 = -1.817 \times 10^{-5}, a_7 = 4.742 \times 10^{-7}, a_8 = 4.244 \times 10^{-9}$$

T and C is temperature ($^{\circ}\text{C}$) and NH_4Cl concentration (wt%) respectively.

The relationship on the liquidus between temperature and composition

$$T(^{\circ}\text{C}) = 4.69 C(\text{NH}_4\text{Cl wt\%}) - 107.7 \quad (C \geq 19.7 \text{ wt\%})$$

$$T(^{\circ}\text{C}) = -0.780 C(\text{NH}_4\text{Cl wt\%}) \quad (C < 19.7 \text{ wt\%})$$

Table 3-2. List of the experimental conditions

Experiment	Initial liquid thickness (cm)	Initial solid thickness (cm)	Mean temperature of Initial solid (°C)	Run duration (min.)
Roof	12.2	10.2	-15.5	150
Floor	12.0	17.0	-16.1	240
Both sides	12.2	Roof : 9.2	Roof: -15.5	260
		Floor: 9.0	Floor: -16.2	

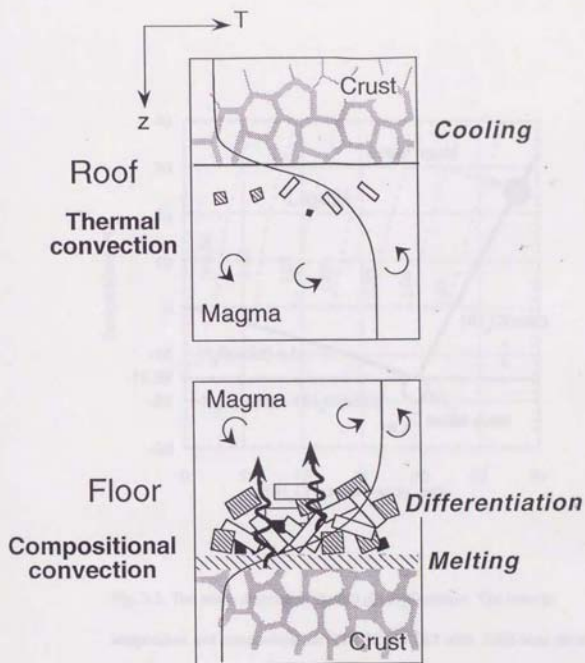


Figure 3.1. The mechanisms of convection at the roof and the floor of the magma chamber

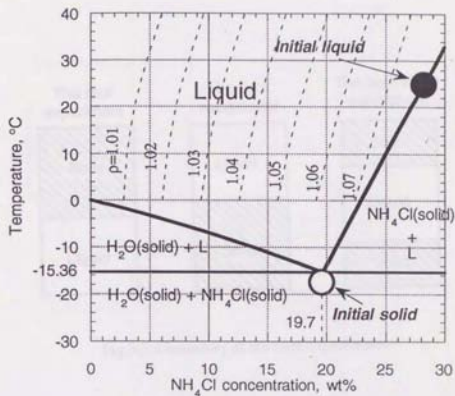


Fig. 3-2. The phase diagram of the NH_4Cl - H_2O system. The eutectic temperature and composition are -15.4 $^{\circ}\text{C}$ and 19.7 wt%. Solid lines show liquidus and solidus, and dashed lines show contour of iso-density of liquid. Filled and open circles show in the initial temperature and composition of the liquid and the solid in the experiments of §3.

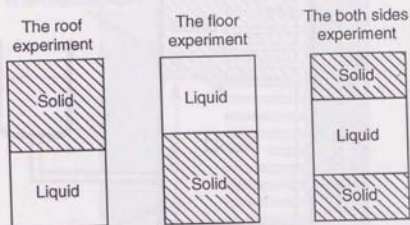


Fig.3-3. Geometry of the three experiments.

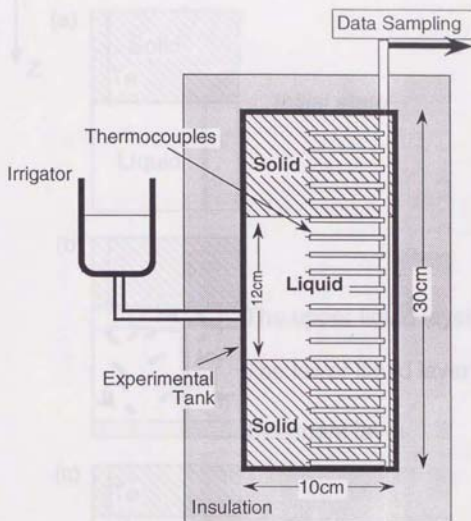


Fig. 3-4. Experimental apparatus. The both sides experiment is shown.

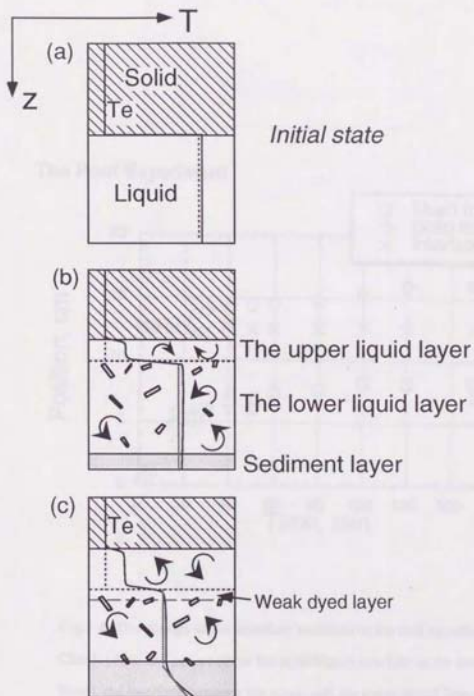


Fig.3-5. The evolution of the system in the roof experiment. The solid and the dashed lines show the temperature and the liquidus profiles. (a) Initial state. (b) Early stage of the roof experiment. (c) After 30 min, weak dyed layer in the lower liquid layer was observed. It was about 1cm thick.

The Roof Experiment

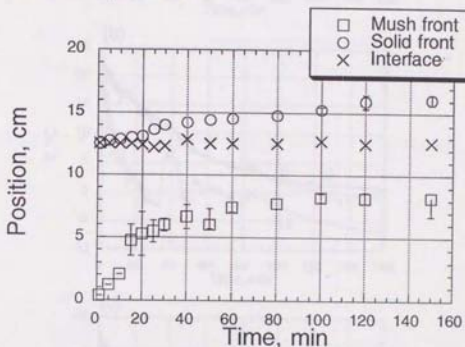


Fig.3-6. The change of the interface positions in the roof experiment.

Circle, cross and square show the solid/liquid interface at the roof (solid front), the interface between the upper and the lower liquid layers and the surface of the sediment layer, respectively.

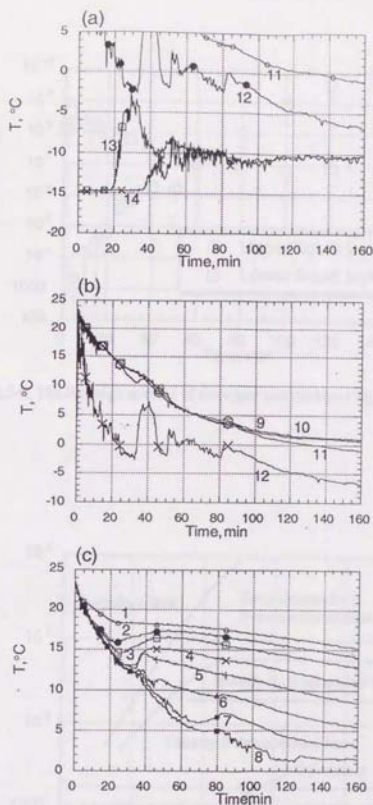


Fig.3-7. The change of the temperature measured at the fixed position in the roof experiment. The figures besides the lines show the height from the bottom of the tank. The interface between the upper and the lower liquid layer was about 12.2 cm high. (a) The upper part near the initial solid front. (b) The middle part. (c) The lower part.

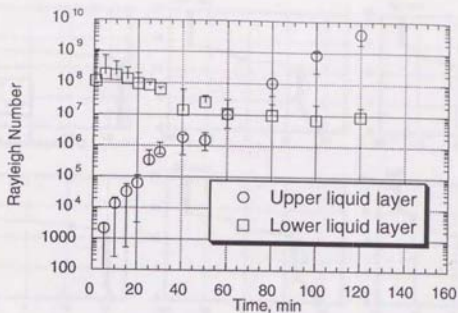


Fig.3-8. The Rayleigh number of the upper and the lower liquid layers.

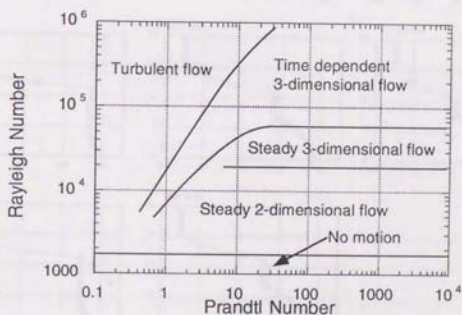


Fig.3-9. Diagram showing the various forms of convection observed in a horizontal layer of liquid, as a function of Rayleigh and Prandtl numbers (Krishnamurti, 1970a,b). The Prandtl number of the liquid in the experiment is 5.8.

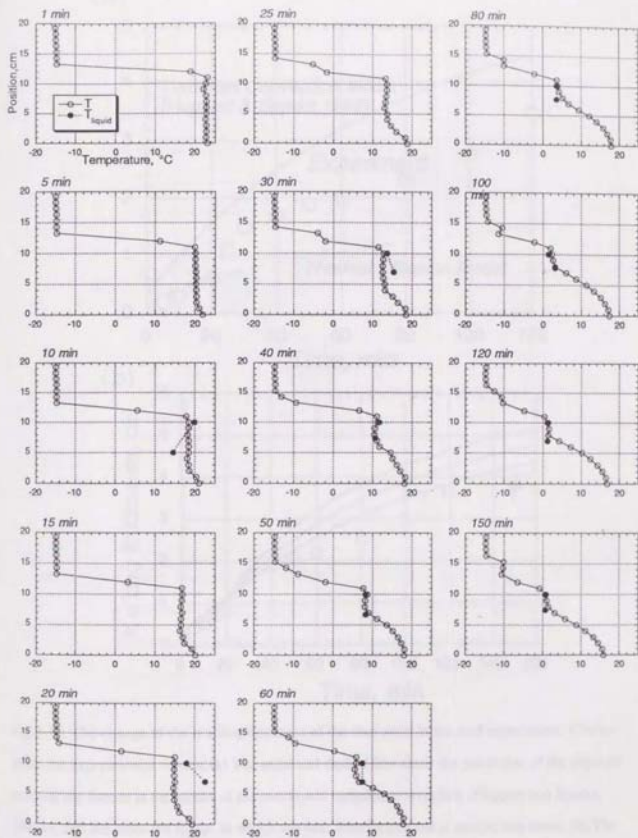


Fig.3-10. Temperature and liquidus profiles in the roof experiment. Temperature (open circle) was measured by the thermocouple. Liquidus (filled circle) is estimated by composition of the liquid.

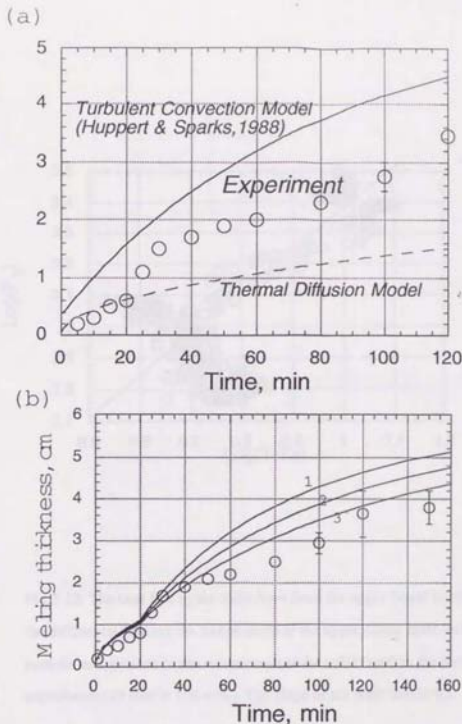


Fig.3-11. The change of the melting thickness of the roof solid in the roof experiment. Circles show the experimental results. (a) The solid and dashed line show the prediction of the physical models; the former is the model of the two layers turbulent convection (Huppert and Sparks, 1988b), and the latter the model in which the heat transfer process is conduction alone. (b) The prediction of the model assuming that the upper liquid layer is stagnant by 20 min and turbulently convective after 20 min. and that the formation of several layers in the lower liquid layer occur. The figures show the number of layers formed in the lower liquid layer.

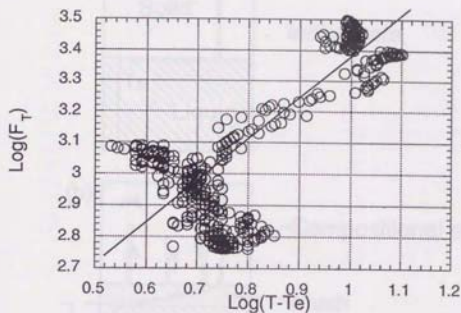


Fig.3-12. The heat flux to the solid front from the upper liquid layer versus the difference between the temperature of the upper liquid layer and the eutectic temperature (= the temperature at the solid front) in the roof experiment (25 min to 100 min.). The slope of the solid line is 4/3.

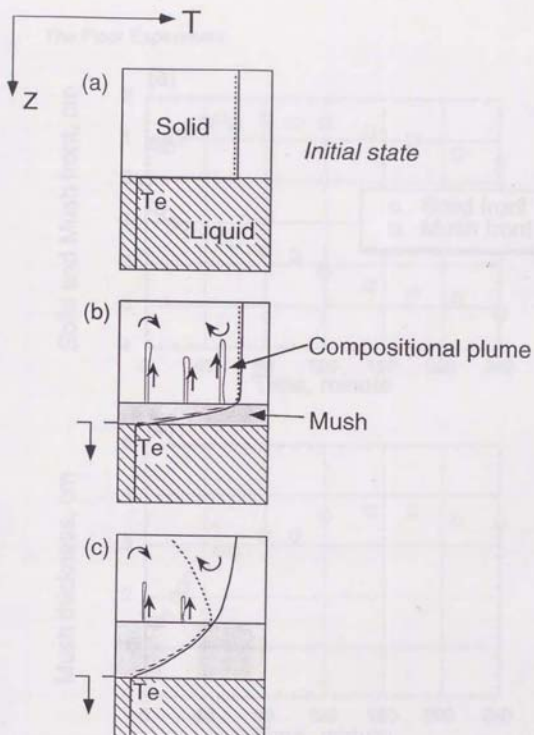


Fig.3-13. The evolution of the system in the floor experiment. The solid and the dashed lines show the temperature and the liquidus profiles. (a) Initial state. (b) Immediately after the experiment started. (c) The liquid became superheated.

The Floor Experiment

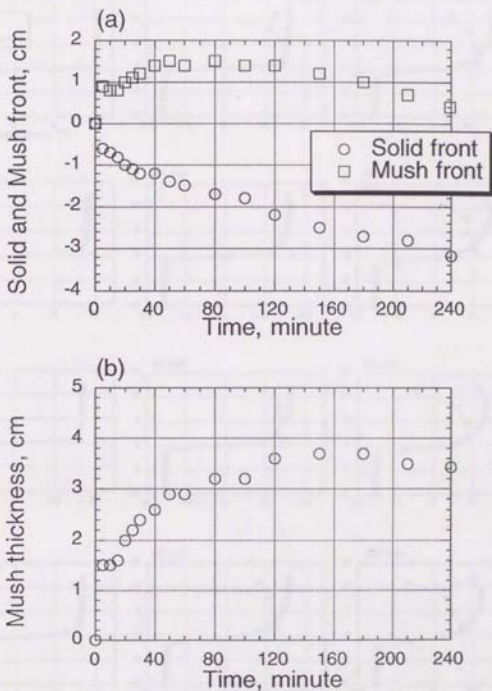


Fig. 3-14. Change of the interface positions and the mush thickness in the floor experiment. (a) Change of the solid and the mush fronts. Circle and square show the solid and the mush fronts, respectively. The base of the position is the initial solid front. (b) The mush thickness.

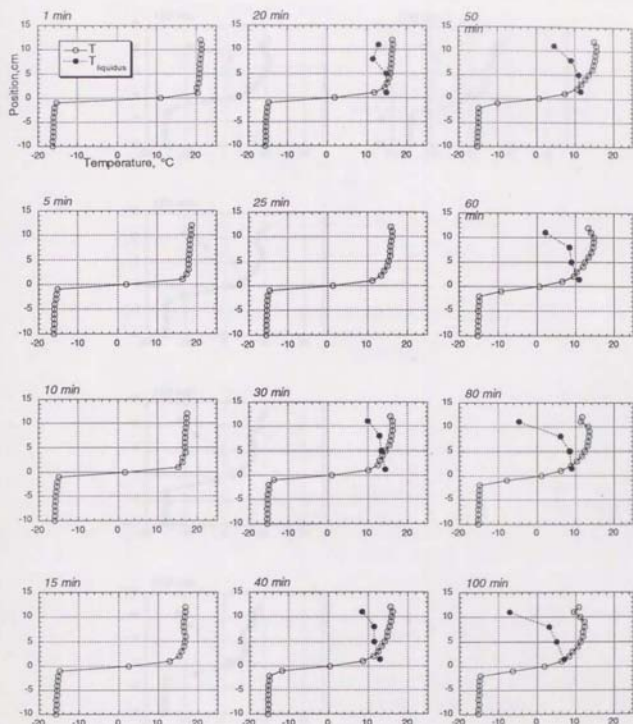


Fig.3-15: Temperature and liquidus profiles in the floor experiment. Temperature (open circle) was measured by the thermocouple. Liquidus (filled circle) is estimated by composition of the liquid.

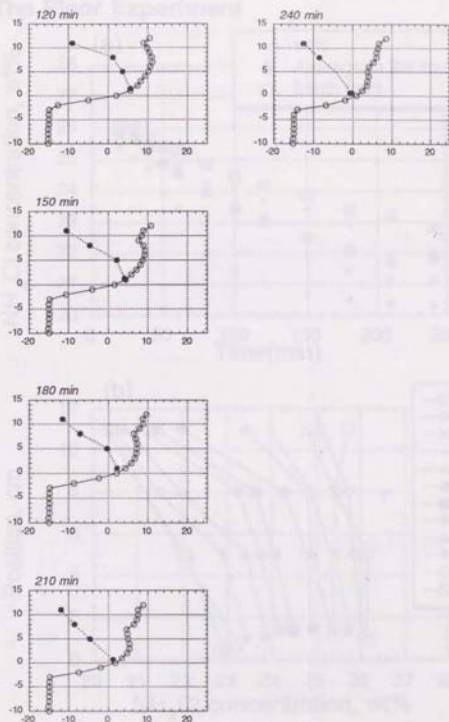


Fig.3-15: Continued.

The Floor Experiment

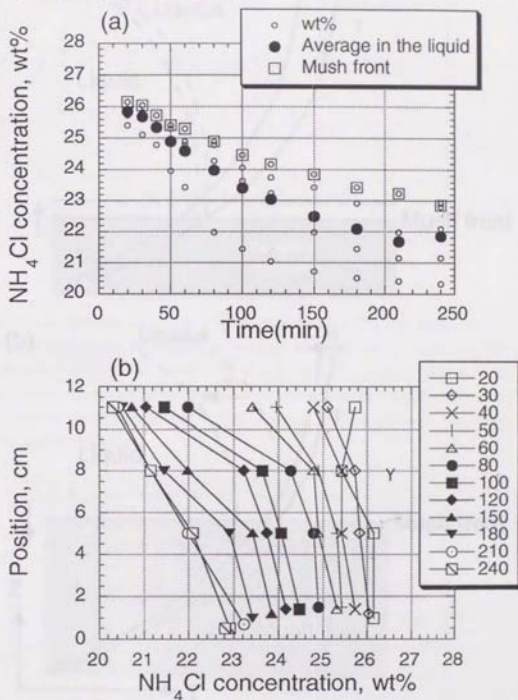


Fig.3-16. Change of the liquid compositions in the floor experiment. (a)

The NH_4Cl content of the liquid versus time. Filled circle, small circle and square show the mean composition, the measured composition and the composition of the mush front, respectively. (b) Change of the

composition profile. The base of the position is the initial solid front. The figures in the legend show time (minute).

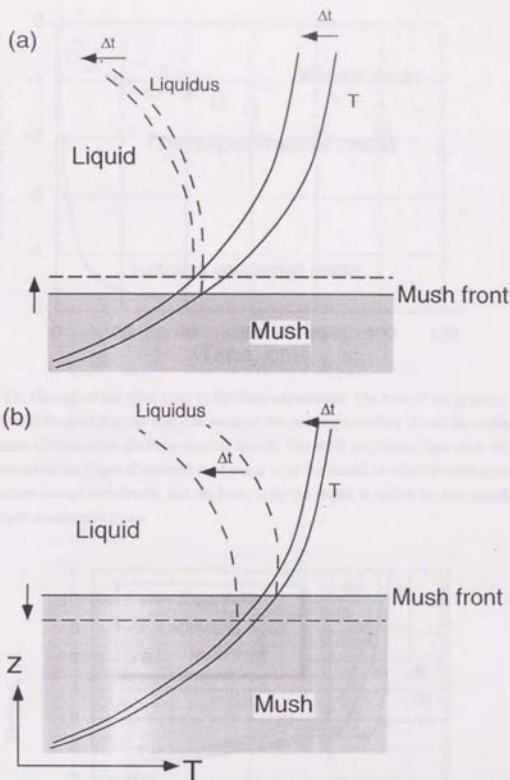


Fig.3-17. Schematic sketch on the migration of the mush front. (a) The case where the mush front migrates upward. The rate of the temperature decrease is larger than that of the liquidus corresponding to the liquid composition. (b) The case where the mush front migrates downward. The rate of the temperature decrease is smaller than that of the liquidus corresponding to the liquid composition.

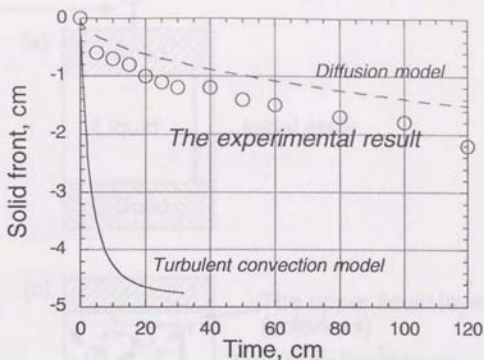


Fig.3-18. Change of the solid front in the floor experiment. The base of the position is the initial solid front so that the absolute value of the melting boundary shows the melting thickness. Circles show the experimental results. The solid and dashed line show the predictions of the physical models; the former is by the model in which the compositional convection occurs turbulently, and the latter is by the model in which the heat transfer process is conduction alone.

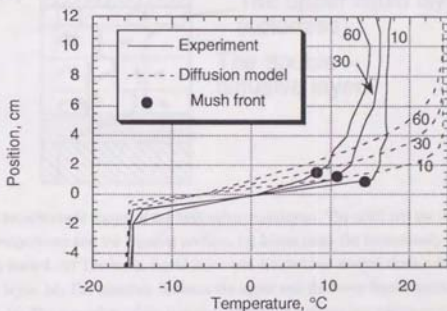


Fig.3-19. Change of temperature profiles in the floor experiment and predicted in the diffusion model. Figures besides lines show the time (minute). Filled circles show the positions of the mush front. The base of the position is the initial solid front.

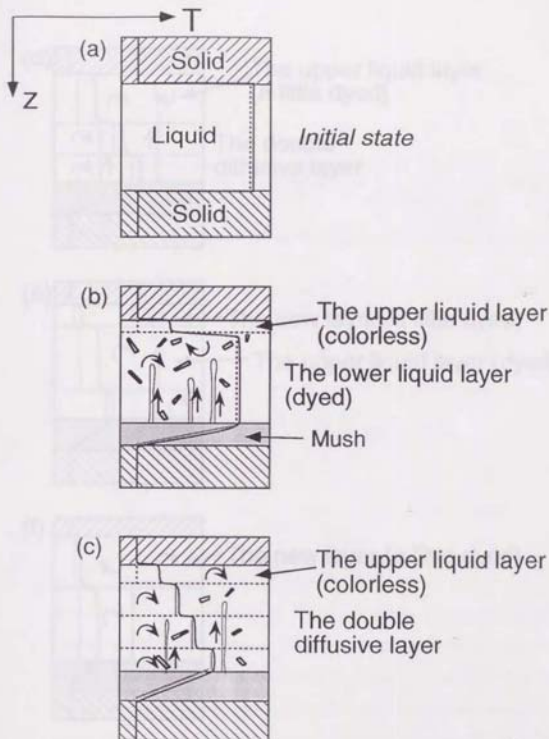


Fig.3-20. The schematic figure of the both sides experiment. The solid and the dashed lines show the temperature and the liquidus profiles. (a) Initial state. (b) Immediately after the experiment started. (c) The lower liquid layer was divided into several double-diffusive convective layer. (d) The interface between the upper and the lower liquid layers migrated downward. (e) The migration of the interface between the upper and the lower liquid layer proceeded. Moreover, the new layer formed near the roof solid. Its interface migrated downward in the similar way to the interface between the upper and the lower liquid layers. (f) The interface between the upper and the lower layers reached the mush front and the lower liquid layer disappeared. The new liquid layer extended to the downward.

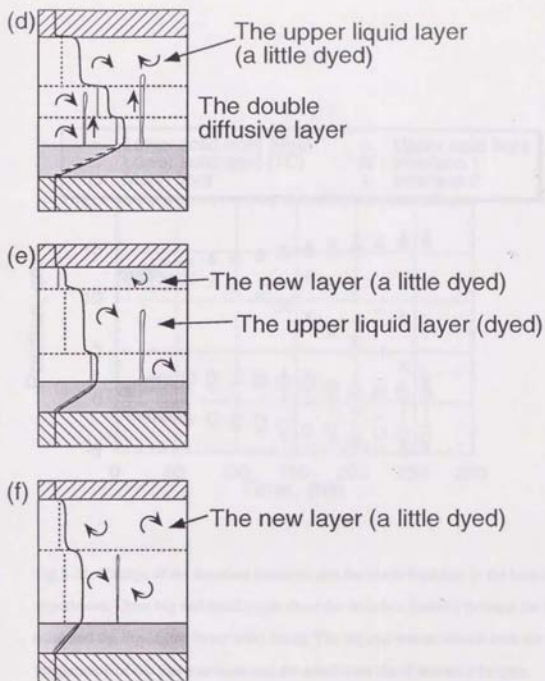


Fig.3-20. (Continued)

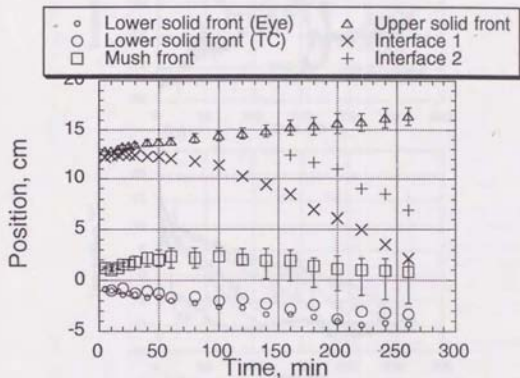


Fig.3-21. Change of the interface positions and the mush thickness in the both sides experiment. Open big and small circle show the interface position between the floor solid and the liquid (the lower solid front). The big one was estimated from the temperature of the thermocouple and the small from the observation by eyes. Square shows the interface between the mush and the liquid (mush front). Triangle shows the interface position between the roof solid and the liquid (the upper solid front). Interface 1 is the interface between the upper and the lower liquid layers and the interface 2 is the new interface (see text). Note that the double diffusive layers in the lower liquid layer are not shown.

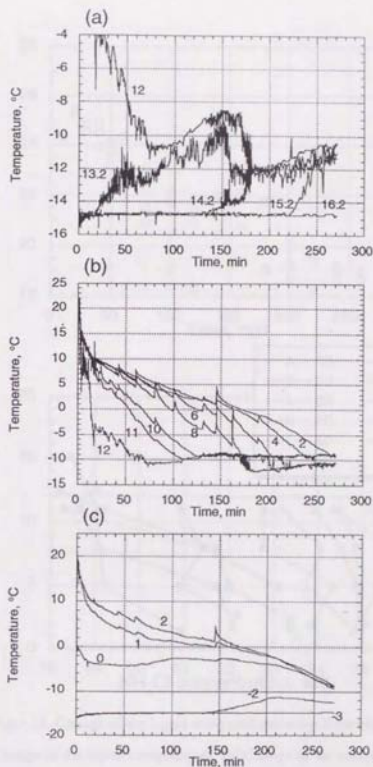


Fig.3-22. The change of the temperature measured at the fixed position in the both sides experiment. The figures besides the lines show the height from the initial lower solid front. The interface between the upper and the lower liquid layer was about 12.2 cm high. (a) The upper part. (b) The middle part. (c) The lower part.

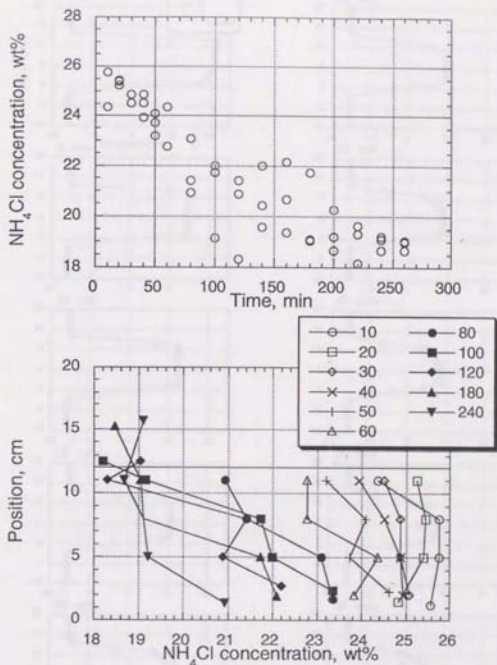


Fig.3-23. Change of the liquid compositions in the floor experiment. (a) Change of the liquid composition. (b) Change of the composition profile. The base of the position is the initial lower solid front. The figures in the legend show time (minute).

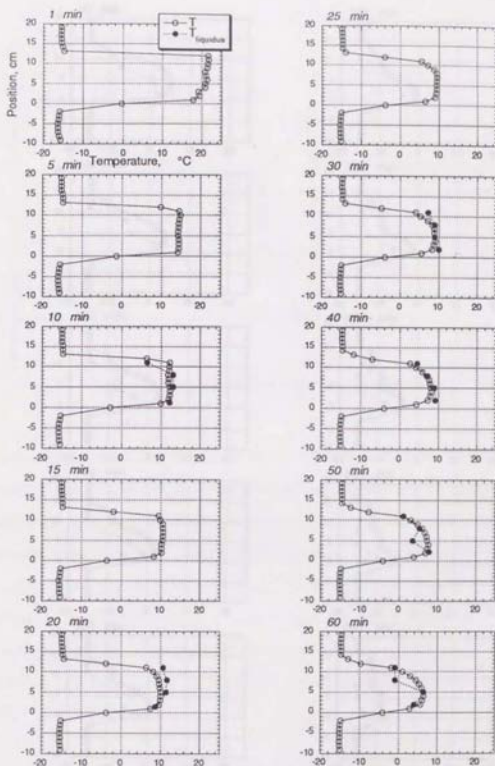


Fig.3-24. Temperature and liquidus profiles in the both sides experiment. Temperature (open circle) was measured by the thermocouple. Liquidus (filled circle) is estimated by composition of the liquid, assumed the thermodynamic equilibrium.

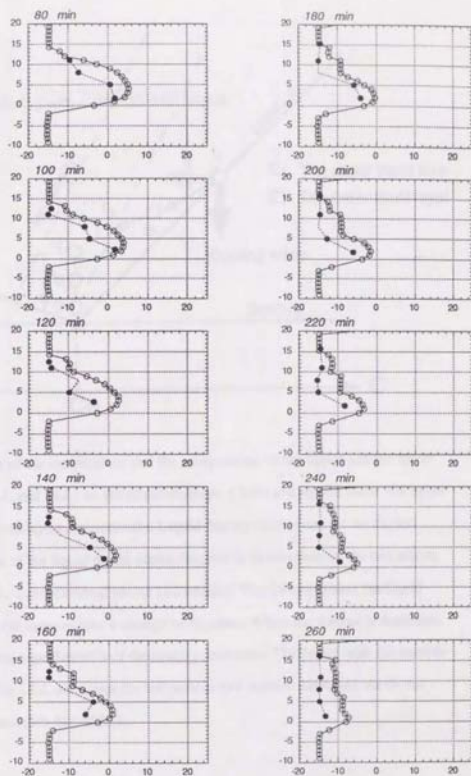


Fig.3-24. (Continued)

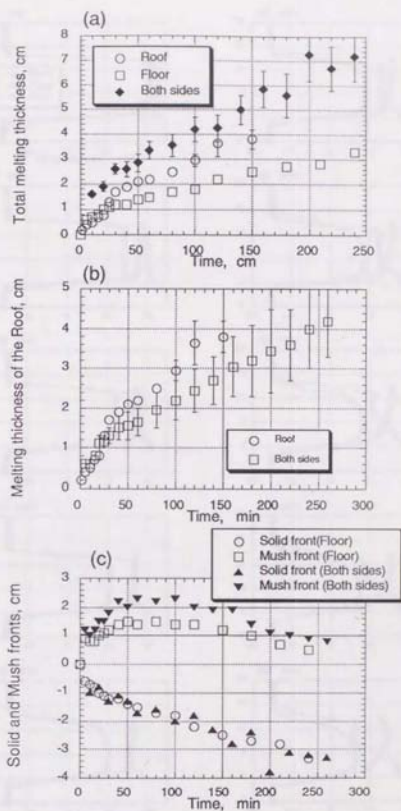


Fig.3-26. Changes of the interface in all experiments. (a) Total melting thickness. (b) Melting thickness at the roof in the roof and the both sides experiments. (c) The mush and solid fronts in the floor and the both sides experiments.

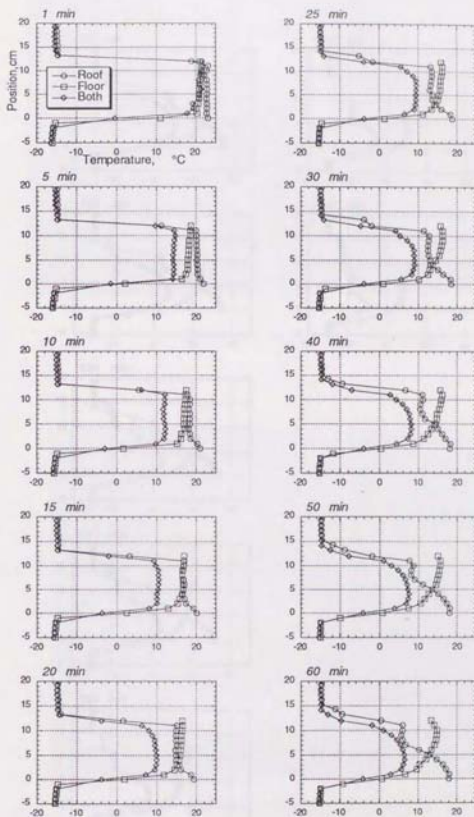


Fig.3-27. Temperature profiles in all experiments. Circle, square and diamond show the roof, the floor and the both sides experiments, respectively. The base of the position is the bottom of the tank in the roof experiment and the initial lower solid front in the floor and the both sides experiments.

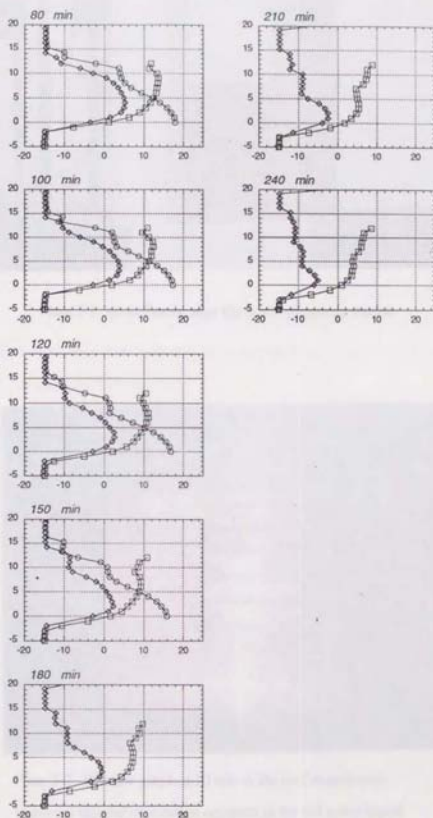


Fig.3-27. (Continued)

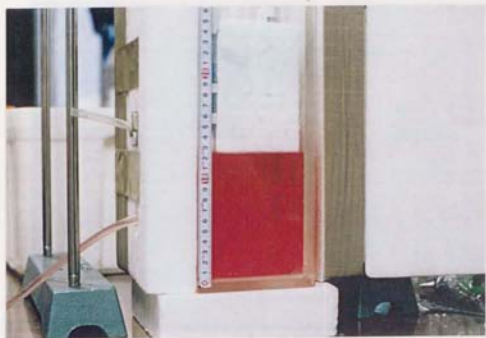


Plate.3-1. Immediately after the roof experiment started.

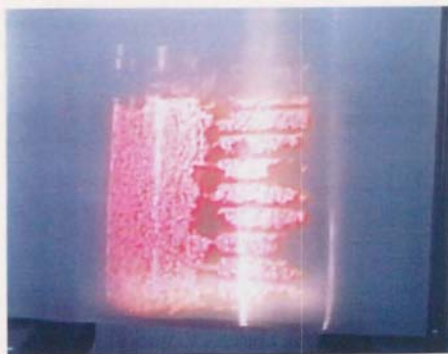


Plate.3-2. Shadow graph at 10 min in the roof experiment.

Vigorous thermal convection occurred in the red lower liquid layer.

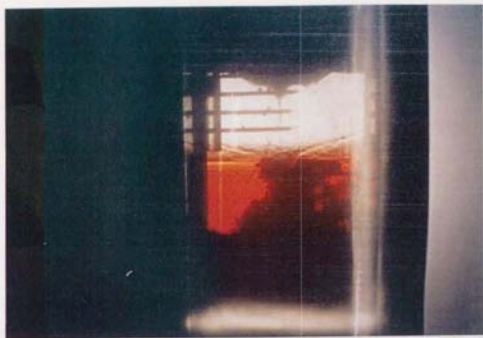


Plate.3-3. The roof experiment at 120 min. The colorless upper liquid layer and the dyed lower liquid layer can be observed. Moreover, the dyed thin layer with about 1cm thick just below the interface between the colorless and dyed regions can be observed.



Plate.3-4. Immediately after the floor experiment started.



Plate.3-5. The floor experiment at 120 min. The mush above the solid front and the conduits in the mush which is called "chimneys" can be observed.

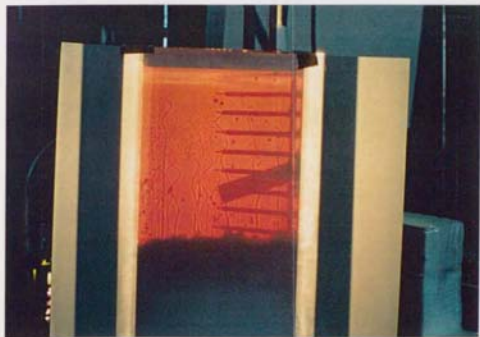


Plate.3-6. Shadow graph at 120 min in the floor experiment. Compositional plumes can be observed.

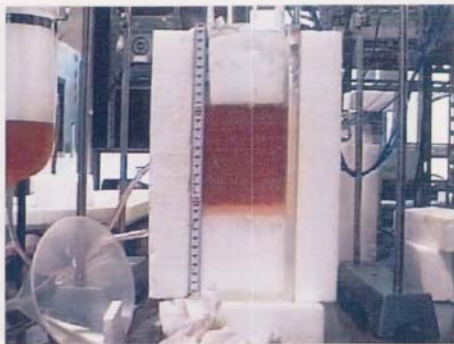


Plate.3-7, Immediately after the both sides experiment started. The formation of the mush above the floor solid can be observed.

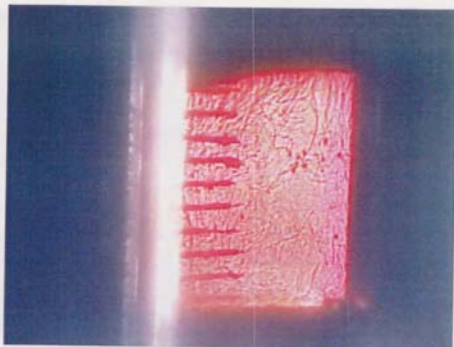


Plate.3-8, Shadow graph at 15 min in the both sides experiment. Thermal and compositional convection occur vigorously.

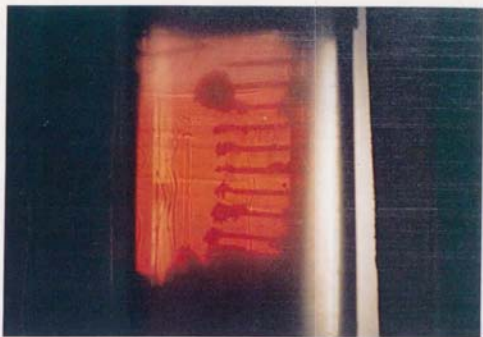


Plate.3-9. The both sides experiment at 80 min. Compositional plumes and double-diffusive layers can be observed. This picture was taken after overturning between the upper and the lower liquid layers, so that the upper liquid layers was little dyed.

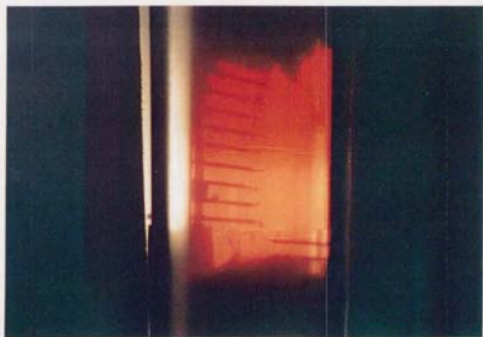


Plate.3-10. Shadow graph at 160 min in the both sides experiment. Three liquid layers can be observed; the top, the middle, and the bottom are the new liquid layer, the upper liquid layer, and the lower liquid layer, respectively.

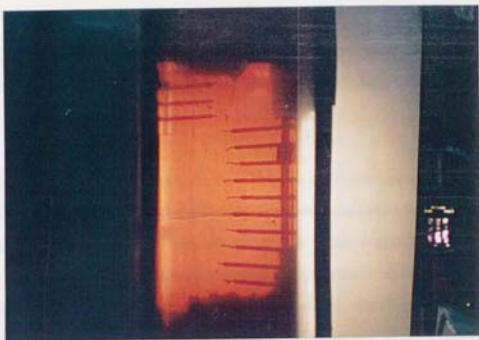


Plate.3-11. Shadow graph at 260 min in the both sides experiment. Two liquid layers can be observed; the upper and the bottom are the new liquid layer and the upper liquid layer, respectively. The interface between the upper and the lower liquid layer reached the mush front, so that the lowr liquid layer did not exist at this time.

4. Analogue Experiments. Part 2 : The Effects of the Composition and the Temperature of the Solid below the Liquid

In the previous section, we can understand the roles of the processes caused at the roof and the floor in the thermal and compositional evolution of the solid-liquid system. The results of the series of the experiments in the previous section suggest that the floor processes are important to the compositional evolution because the compositionally unstable melt generated by the floor solid and liquid released by crystallization mix with the overlying liquid and make its composition change. In this section, I present the results of another series of analogue laboratory experiments to understand the compositional evolution due to the change of the conditions of the crust. The composition and the temperature of the floor solid are focused upon in this section.

4.1. Experimental technique and condition

Initial condition

The experiments have been carried out in the various initial conditions of the solid. The two series of the experiments will be presented in this section: one series is that the solid compositions were systematically changed and the other is that the initial solid temperature were changed. The conditions varied in the experiments were the initial solid composition and the initial solid temperature. All experiments are compared with the floor experiment carried out in §3.3, in which the solid composition was the eutectic and the initial temperature of the solid was slightly below the eutectic temperature. The list of the experiments presented in this section is shown in Table 4-1.

Apparatus and procedures

The experimental apparatus was the same as the floor experiment in §3. Procedures were also similar. The used tank, the methods of observation and the measurement of the temperature and the composition profiles are the same as those described in §3.1.

In this series of the experiments, the conditions of the floor solid were changed. The initial temperature of the solid can be changed easily. On the other hand, the various compositions of the solid mixture cannot be made easily. We can easily make only the solid with the eutectic composition by cooling of NH_4Cl solution with the eutectic composition because the phase change from liquid to solid occurs completely at the eutectic temperature. However, the solution with non-eutectic composition makes the liquid composition change during solidification. Then the liquid density changes during solidification and compositional convection occurs. Thus, we cannot make the homogenous solid mixture in composition easily. In order to make it, I need to avoid the onset of the compositional convection.

I used three solid compositions, the eutectic, 28 NH_4Cl wt% and 73 NH_4Cl wt% in the experiments. I made 28wt% solid in the following method. The aqueous solution of 28wt% was prepared in the first step. 2 cm^3 of the aqueous solution was poured in the tank cooled strongly (-50°C) in every 20 min. The solution of 2 cm^3 was 2 mm high in tank. The solution quenched and the convection would not occur. 73wt% solid was made in the following method. Enough NH_4Cl fine crystals and water were mixed. The interstitial liquid in the NH_4Cl solid would be saturated. This mixture was poured in the tank and cooled strongly. The permeability of the mixture would be small and it was expected that convection did not occur. After solidification, the compositional profile in the solid made in this way were tested. The heterogeneity of the composition was within $\pm 2\text{ wt\%}$.

4.2. The effect of the composition of the solid

The experiments using the solids with three compositions carried out to investigate the effects of the solid composition on the evolution of the solid-liquid system (Fig.4-1).

The composition of the solid in the binary eutectic system changes the degree of partial melting at the eutectic temperature. As the NH_4Cl content of the solid increases, the degree of partial melting at the eutectic temperature decreases (Table 4-2).

The evolution in the experimental systems was similar to that of the floor experiment described in §3.3. However, the origins of the mush were much different between the solid with the eutectic composition and others. The solid with the eutectic composition melts completely at the eutectic temperature. Thus the mush was formed only by crystallization from the liquid. On the other hand, the solid with higher NH_4Cl content than the eutectic partially melts at the eutectic temperature. Thus there are two origin of the mush: one is generated by crystallization and the other is generated by partial melting of the solid. The former was the mush above the initial solid/liquid interface (the solid front) and the latter was the mush below the initial solid front. Compaction of the mush was not observed in the experiments.

The mush generated by partial melting of the colorless solid became dyed (Fig. 4-2). This fact indicated that the liquid above the initial solid front penetrated into the mush generated by partial melting of the solid. Change of the bulk compositional profile in the experiment using 28 wt% solid is shown in Fig. 4-3. The dashed lines show the bulk composition estimated from mass balance. For estimation, it is assumed that the compositional profile is linear in the mush. The circulation of the interstitial liquid of the mush makes the composition in the original solid region become higher NH_4Cl content.

The intensity of the compositional convection, the solid front, the mush fronts, the mush thickness and the liquid composition systematically changed in the variation of the solid composition. As the NH_4Cl content of the solid mixture increased, the compositional convection became weaker (Plates 4-1, 4-2, 4-3 and 4-4), the migrations of the solid and the mush fronts became rapid and the rate of the compositional decrease of the liquid became smaller (Figs. 4-4 and 4-5). Nevertheless, the temperature profiles were roughly similar (Figs. 4-6, 4-7, and 4-8).

The migration rate of the solid front increased as the NH_4Cl content of the solid increased (Fig. 4-4). Because the solid temperature was near the eutectic temperature, the

heat flux from the solid front to the solid was negligible. Thus, the heat flux from the mush to the solid front could be estimated from the migration rate of the solid front. The heat flux F_T from the mush to the solid front is expressed by

$$F_T = -\rho L(1 - \phi_e) \frac{da}{dt} \quad (4-1)$$

where ρ , L , ϕ_e and a are the density of the solid, latent heat, the solid fraction at the eutectic temperature and the position of the solid front. This heat flux was proportional to the migration rate of the solid front. As the NH_4Cl content of the solid used in the experiments increased, F_T decreased, although the migration rate of the solid front increased. This mechanism will be discussed later.

Let us consider the change of the liquid composition. The evolution of the liquid composition is caused by mixing with the two kinds of low NH_4Cl content liquids: one is the melt generated by melting of the solid and the other is the interstitial liquid within the mush. Now the compositional flux F_C is defined as

$$F_C = -H \frac{dC}{dt} \quad (4.2)$$

where H and C are the liquid thickness and the liquid composition. This compositional flux is the absolute decreasing rate of the chemical species (in this case, NH_4Cl). This compositional flux can be divided into two contributions of the melt of the solid and the interstitial liquid in the mush. Thus we can write

$$F_C = F_{C(\text{melt})} + F_{C(\text{mush})} \quad (4.3)$$

The melt of the solid melted at the eutectic temperature had the least NH_4Cl content in the experimental system and the least density below the mush front. I assume that the melt of the solid perfectly rises up and mixes with the overlying liquid. Then $F_{C(\text{melt})}$ can be written

$$F_{C(\text{melt})} = (C - C_e) \frac{da}{dt} \quad (4.4)$$

where C_e is the eutectic composition. Under this assumption, $F_{C(\text{mush})}$ can be estimated as

$$F_{C(\text{mush})} = F_C - F_{C(\text{melt})} \quad (4.5)$$

because F_C and $F_{C(\text{melt})}$ can be estimated from the results of the experiment. The changes of $F_{C(\text{melt})}$ and $F_{C(\text{mush})}$ are shown in Fig.4-10. Both compositional fluxes decreased as

the NH_4Cl concentration of the solid increased. Both processes of melting of the solid and rising up of the interstitial liquid of the mush became less effective on the compositional evolution of the system.

I consider the mechanism of the systematic change of the evolution of the experimental system caused by the composition of the solid. As the NH_4Cl concentration of the solid increased, the degree of partial melting of the solid at the eutectic temperature decreases and hence the heat required to migrate the solid front decreases. Thus the more rapid migration of the solid front occurs as the NH_4Cl concentration of the solid increased. This rapid migration causes the temperature profile at the solid front in the liquid side (in the mush) relax (Fig.4-10). Thus the heat flux to the solid front from the mush decreased. Namely, as the NH_4Cl content of the solid increased, the production rate of the melt generated by melting of the solid that is the least NH_4Cl content becomes smaller. This mechanism causes $F_{C(\text{melt})}$ decrease. Moreover, as the NH_4Cl concentration of the solid increased, the partially molten solid increased in solid fraction at the eutectic temperature. This increasing of the solid fraction causes the mush become low porosity and hence low permeability. Thus compositional convection becomes weaker and the interstitial liquid in the mush cannot easily separate from the mush and mixes with the overlying liquid. This mechanism causes $F_{C(\text{mush})}$ decrease. The slow evolution of the composition of the liquid makes the mush front high because the liquidus temperature is high.

4.3. The effect of the initial temperature of the solid

The experiments using two initial temperatures of the solid were carried out to investigate the effects of the temperature of the crust on the evolution of a magma system. The warm (-16.1°C) and the cold (-44°C) solids were used (Fig.4-1). The compositions of the solid were the eutectic in both two experiments (Table.4-2). The evolution in the experimental system was similar to that of the floor experiment described in §3.3.

The melting rate was smaller in the experiment using the cold solid than in the experiment using the warm solid (Fig.4-12a). It was observed that the compositional convection was less vigorous, the mush front was higher (Fig.4-12a), the mush thickness was larger (Fig.4-12b), and the decrease of the NH_4Cl content of the liquid was slower (Fig.4-13a) in the experiment of the cold solid. The relationship of the temperature and the compositional profiles in the experiment of the cold solid were qualitatively similar to that of the warm solid (Fig.4-14).

The colder the solid became, the more the heat loss from the liquid into the solid became. Thus the ratio of the heat flux used to melt the solid to the heat flux from the mush to the solid front decreased. As the initial temperature of the solid decreased, the production rate of the melt generated by the solid decreased. Therefore, the decrease of the NH_4Cl content of the liquid became slower as the solid becomes colder. The slow decrease of the NH_4Cl content of the liquid made the position of the mush front become high because the liquidus temperature is high although the temperature profiles does not change largely (Fig.4-15).

The liquid temperature in the experiment using the cold solid had more gradient than that in the experiment using the warm solid. The less production rate of the melt in the experiment of the cold solid causes compositional convection less vigorous. Although the compositional convection generally carries a low heat flux, the intensity of the compositional convection would make this difference of the temperature profiles

4.4. Summary

The NH_4Cl contents of the solids were systematically changed in the experiments. The solid fraction at the constant solidus (the eutectic temperature) increases as the NH_4Cl content of the solid increases. The results of the experiments systematically changed in the following two points. (i) The migration rate of the solid front increased and (ii) the decrease of the NH_4Cl content of liquid became slower as the NH_4Cl content of the solid increased. The reason of (i) is that the heat required to migrate the interface

decreases as the solid fraction increases with the NH_4Cl content of the solid. The reasons of (ii) are that the production rate of the melt with the eutectic composition generated by melting of the solid at the solid front decreased because the solid front migrated rapidly and hence the temperature gradient above the solid front decreased and that the compositional convection becomes less vigorous because the solid fraction of the partial molten crust increases and the permeability in the mush decreases.

The melting rate of the solid decreased and the decrease of the NH_4Cl content of the liquid became slower as the initial temperature of the solid became colder. These are because increase of the heat loss into the solid caused the amount of the melt with the eutectic composition generated by melting of the solid decrease and it caused the decrease of the NH_4Cl contents of the liquid become slow, as the temperature of the solid became colder.

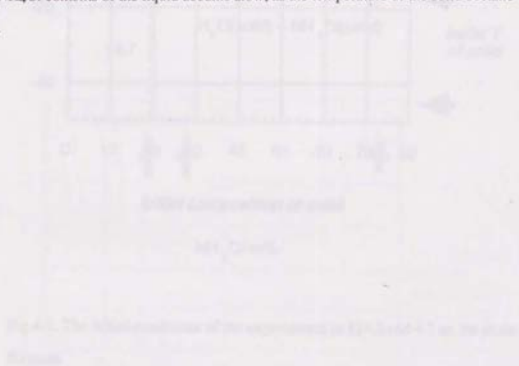


Fig. 4.1. The relationship of the composition of the solid and the initial temperature of the solid.

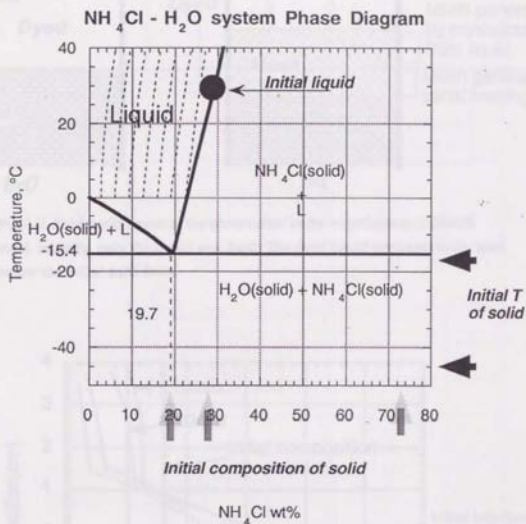


Fig.4-1. The initial conditions of the experiments in §§4.2 and 4.3 on the phase diagram.

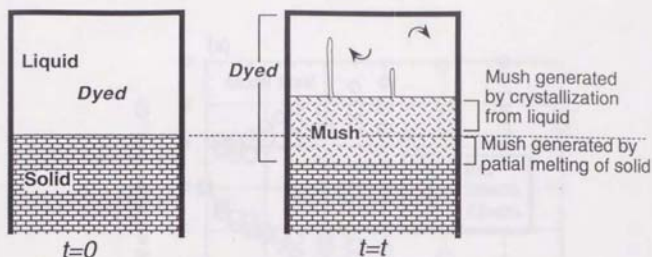


Fig.4-2. Schematic figure of the observation in the experiments of 28wt% solid. Initially, only the liquid was dyed. The dyed liquid penetrated to the level below the initial solid front.

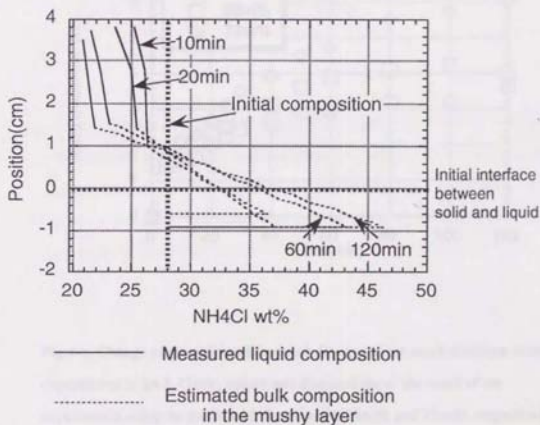


Fig.4-3. Change of the bulk compositional profile in the experiment using 28wt% solid. The compositional change not only the liquid but also the original solid region.

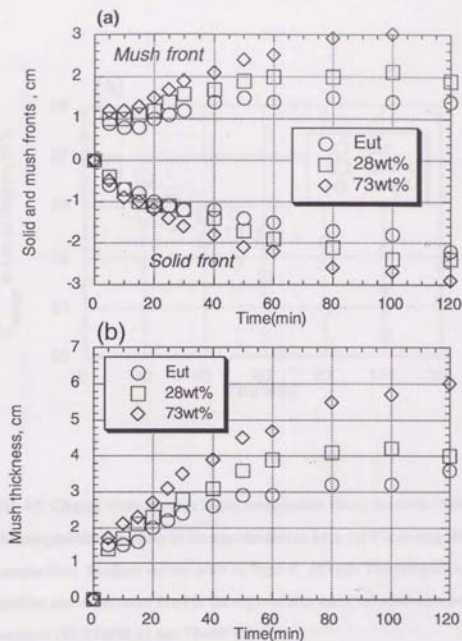


Fig.4-4. Change of the solid and the mush fronts and the mush thickness in the experiments in §4.2. Circle, square and diamond show the result of the experiments using the solids with the eutectic, 28wt% and 73wt%, respectively.
 (a) The solid and the mush fronts. (b) The mush thickness.

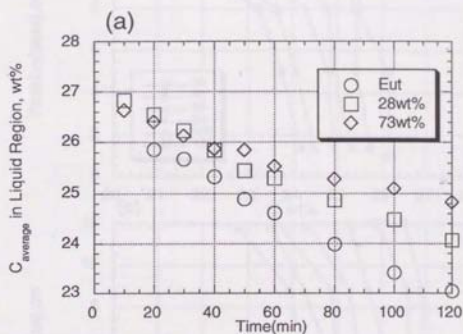


Fig.4-5. Change of the average liquid composition above the mush front and the compositional profiles in the experiments in §4.2. (a) The average liquid composition. Symbols are the same as Fig.4-4. (b)-(d): The compositional profiles above the mush front in the experiments using the solid with the eutectic (b), 28wt% (c) and 73wt% (d).

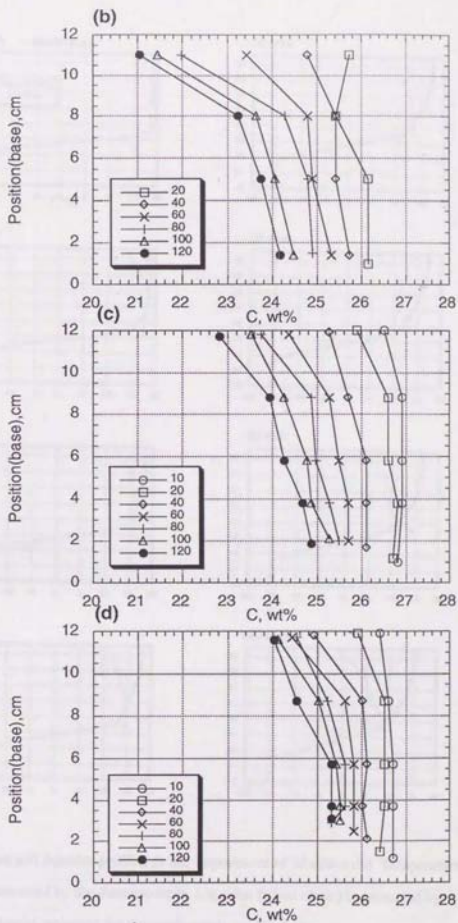


Fig.4-5. (Continued)

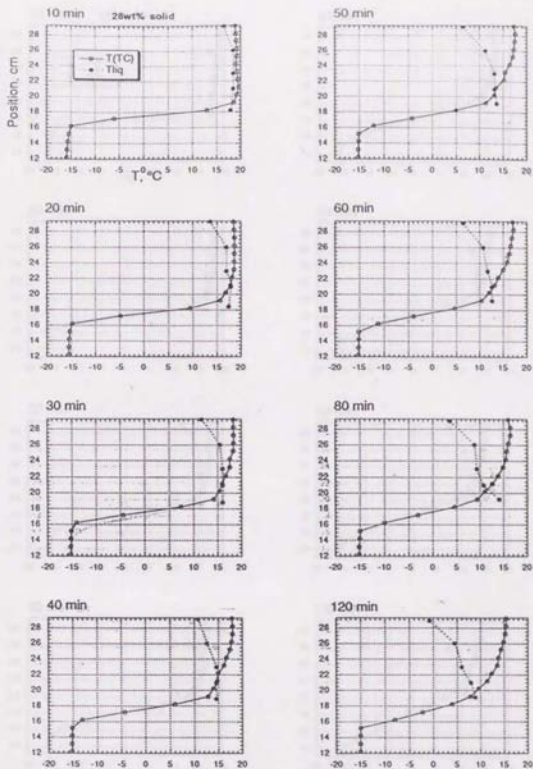


Fig.4-6. Temperature and liquidus profiles in the experiment of 28wt% solid. Temperature (open circle) was measured by the thermocouple. Liquidus (filled circle) is estimated by composition of the liquid, assumed the thermodynamic equilibrium.

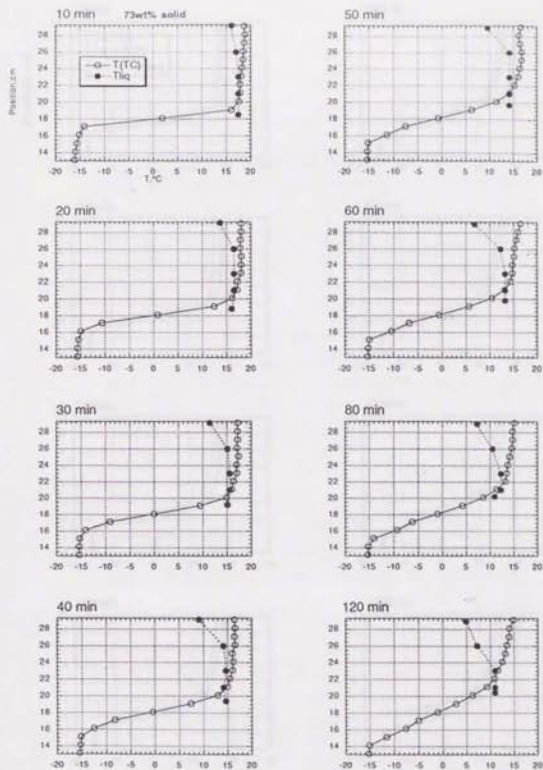


Fig.4-7 Temperature and liquidus profiles in the experiment of 73wt% solid. Temperature (open circle) was measured by the thermocouple. Liquidus (filled circle) is estimated by composition of the liquid.

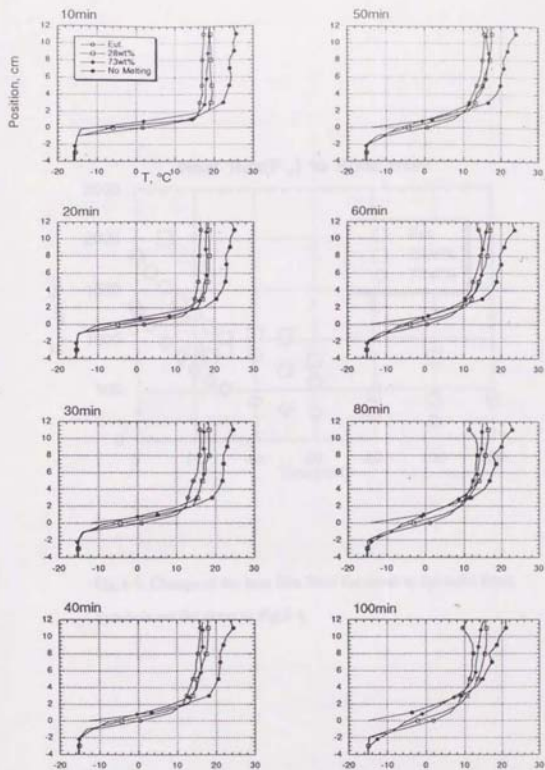


Fig.4-8 Temperature profiles in the experiments of the eutectic(circle), 28wt%(square) and 73wt%(diamond) solid.

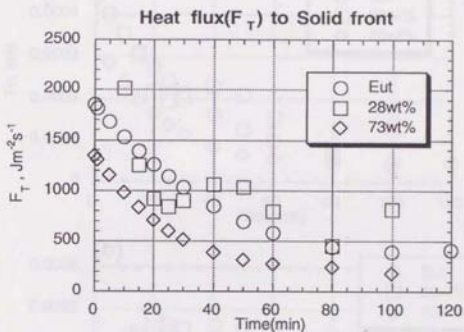


Fig.4-9. Change of the heat flux from the mush to the solid front.
Symbols are the same as Fig.4-4.

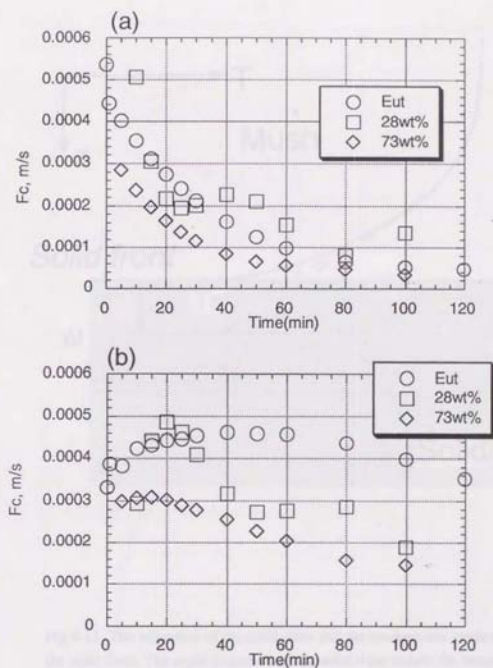


Fig.4-10. Changes of the compositional fluxes in the experiments in §4.2.
 Symbols are the same as Fig.4-4. (a) The compositional flux caused by melting of the solid. (b) The compositional flux caused by rising up of the interstitial liquid in the mush.

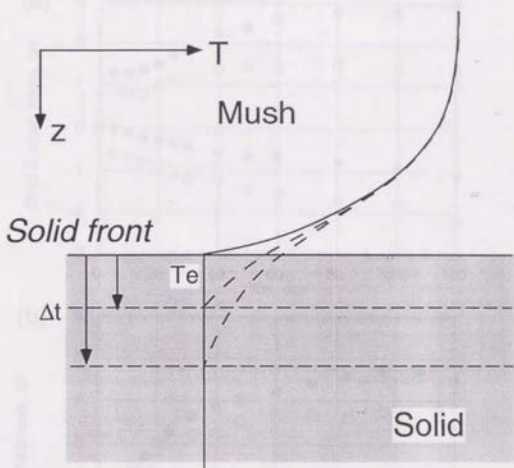


Fig.4-11. The migration of the solid front and the temperature gradient above the solid front. The rapid migration of the solid front causes the temperature gradient become small.

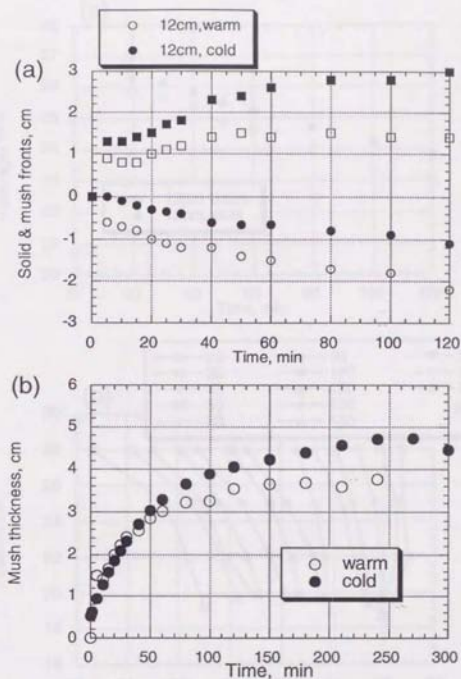


Fig.4-12. Change of the solid and the mush fronts and the mush thickness in the experiments in §4.3. Open and filled symbols show the experiments of the warm and the cold solids, respectively. (a) The solid (circle) and the mush (square) fronts. (b) The mush thickness.

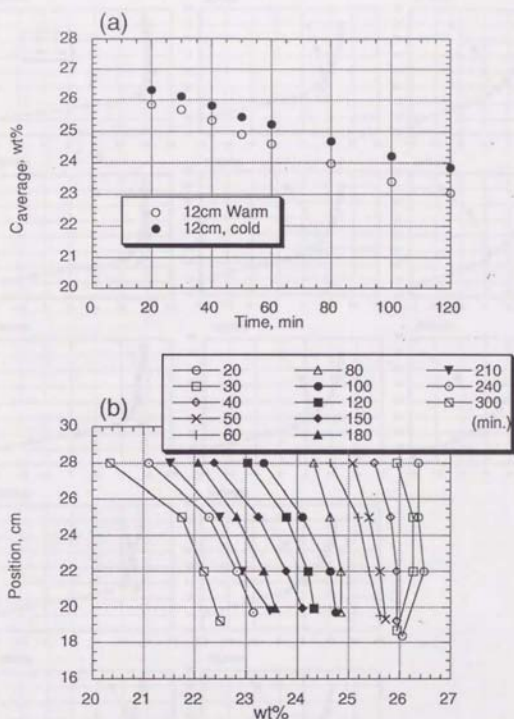


Fig.4-13. Change of the average liquid composition and the compositional profiles in the experiments in §4.3. (a) The average liquid composition. Open and filled symbols show the experiments of the warm and the cold solid, respectively. (b) The compositional profiles in the experiment of the cold solid.

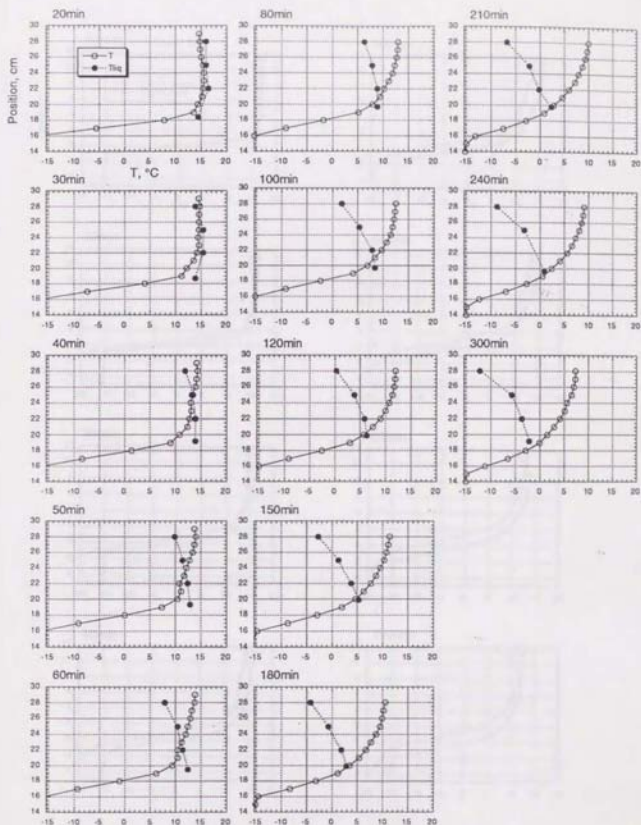


Fig.4-14 Temperature and liquidus profiles in the experiment of cold solid. Temperature (open circle) was measured by the thermocouple. Liquidus (filled circle) is estimated by composition of the liquid, assumed the thermodynamic equilibrium.

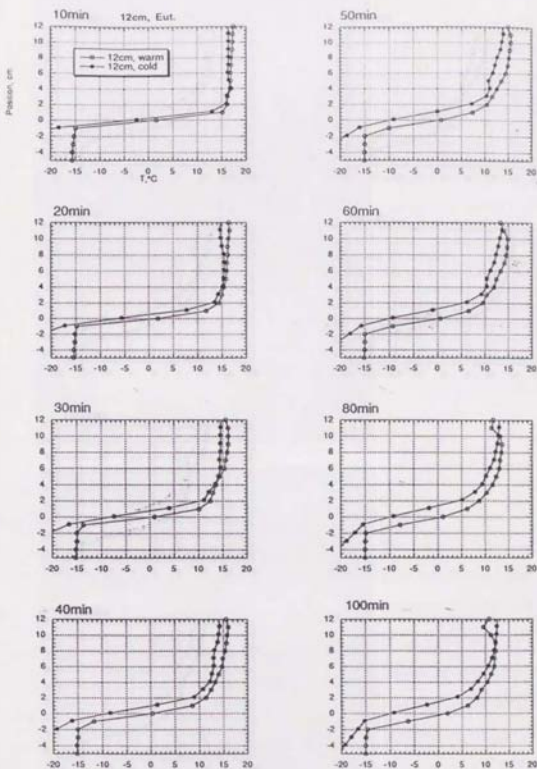


Fig.4-15 Temperature profiles in the experiments using the warm (open circle) and the cold (filled circle) solids.

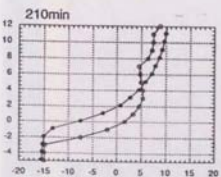
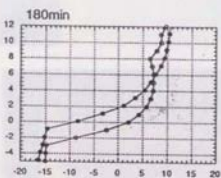
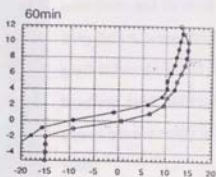
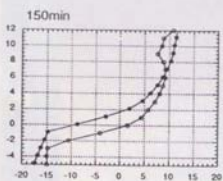
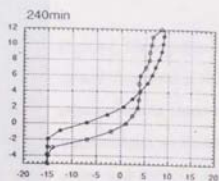
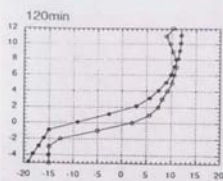


Fig.4-15. (Continued)

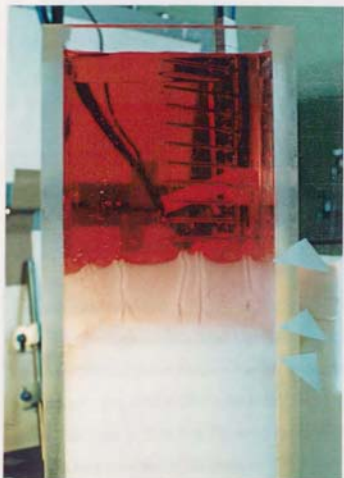


Plate.4-1. The experiment using 28 wt% floor solid at 120 min. 5 chimneys can be observed. 3 white triangles are the positions of the mush front, the initial solid front, and the solid front, from the top, respectively. The mush below the initial solid front was dyed, although it cannot be seen easily in this plate.



Plate.4-2. Shadow graph at 120 min in the experiment using 28 wt% floor solid. Upwelling compositional plumes from the mush front can be observed.

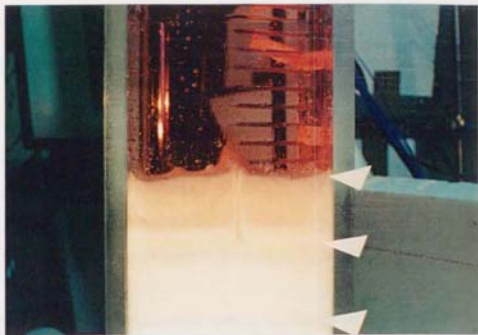


Plate.4-3. The experiment using 73 wt% floor solid at 120 min. A chimney can be observed. The number of chimneys in this experiment was less than that in the experiment using 28wt% floor solid at the same time (Plate.4-1). 3 white triangles present the same as Plate.4-1. The mush below the initial solid front was dyed, although it cannot be seen easily in this plate.

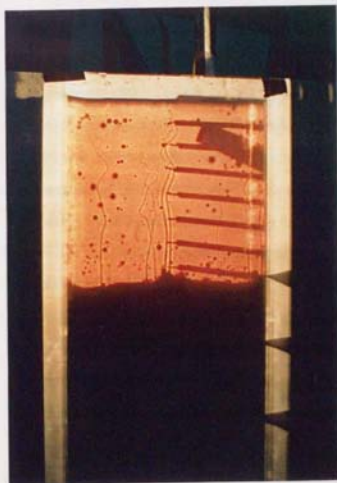


Plate.4-4. Shadow graph at 120 min in the experiment using 73 wt% floor solid. Upwelling compositional plumes from the mush front can be observed. The number of the plumes was less than that in the experiment using 28 wt% floor solid at the same time (Plate.4-2).

5. Implication to a Natural Magma System

I give a discussion of possible applications to natural magma systems that occur in the Earth on the basis of the results of the theoretical analysis and the analogue experiments.

5.1. The evolution of the magma system for a single intrusive event

The roles of the processes at the roof and the floor of the magma chamber

The results of the experimental study suggest that the heat flux to the roof crust from the underlying magma is determined by the thermal convection and is given by equation (2-3a) and that the heat flux to the floor of the chamber is not effectively carried by the compositional convection. Therefore, the processes at the floor would not contribute to the rapid cooling of the magma in the magma chamber.

The melt generated by melting of the roof crust would hardly mix with the underlying original magma. On the other hand, the melt generated by melting of the floor crust would rise up and effectively mixes with the overlying original magma. The compositional convection caused by the floor melting of the magma chamber is important to the compositional evolution of the magma. In particular, when the number of the components of the system is more than 3, mixing of the compositional plume of the melt of the crust and the interstitial liquid in the mush greatly modifies the liquid line of descent of the original magma.

The chemical differentiation of the magma would also proceed due to mixing with the compositional plumes by the two independent modes of the convective instabilities in the mush, which are that of the thin chemical boundary layer near the interface between the mush and the magma and that of the interstitial liquid within the mush (e.g. Tait and Jaupart, 1989, 1992; Worster, 1992). The liquid line of descent of the magma would be modified in different ways due to the two modes of the convective instabilities. The compositional plumes by the former instability have the composition near the magma. On

the other hand, the compositional plumes by the latter instability can have the various compositions ranging from the composition near the magma to the composition at the solidus. Therefore, the latter instability is more important to the modification of the liquid line of descent of the magma than the former one. This mode approximately corresponds to the boundary crystallization proposed by Langmuir (1989). It is reported in the previous experiments on crystallization of the liquid cooled from below that the former instability can occur first, followed by the latter (e.g. Chen et al., 1993). In the floor and the both sides experiment in this thesis, it was observed that the rising compositional plumes like one of the latter instability occurred immediately after the experiments started. These plumes would be caused by the buoyant melt generated by the roof solid. In this case, the fluid motion within the mush would be changed by the plumes by the melt of the floor solid which pass through the mush from the early stage. When melting of the floor crust causes the fluid motion of the interstitial liquid within the mush change, this change may affect the liquid line of descent and the magma and petrographical features of the cumulate rocks. The further investigation on this problem is required.

The results of the experiments suggest that the compositional gradient generated by the compositional convection enhances the formation of double diffusive layers in the magma chamber. The formation of double diffusive layers decreases the upward heat flux because the more layers there are over a given depth, the smaller are the temperature steps between them, and hence the smaller the heat flux.

Time scale of the rapid cooling stage

The results of the numerical calculation (§2) suggest that the magma system has the two cooling stages: one is the rapid cooling stage and the other is the slow cooling stage. Whether the magma system is in the rapid cooling stage or in the slow cooling stage is determined by whether the crust melts by the vigorously convective heat flux or not. When this criterion is applied to the magma system, it is concluded that the evolution of the magma system in the rapid cooling stage occurs only in the case in which the melting temperature of the roof crust is lower than the temperature of the magma.

Let us consider a hot magma (for example, basaltic magma) is emplaced in a crust of the lower EFT than the temperature of the magma (for example, granitic to dioritic crust). This would be the most common case. When the hot magma is supplied into the crust, the crust is heated up and hence begins to melt when the interface temperature becomes its EFT, followed by generation of the silicic magma. This silicic magma will form a separate layer not to mix with the original magma. The amount of the silicic magma increases and the temperatures of both the magmas decrease with time rapidly as far as the temperature of the silicic magma is larger than its EFT (the rapid cooling stage). When the silicic magma decreases in temperature to near its EFT, rapid melting of the crust ceases and the magma system begins to evolve in the slow cooling stage.

Time at which the magma system with 1000 km thick magma is in the rapid cooling stage is, for example, about 100 years when the magma convects as one or two layers. However, the compositional gradient generated by the compositional convection is expected to enhance the formation of the double diffusive layers in the magma. The formation of the double diffusive layers causes the upward heat flux decrease and the temperature decrease of the magma becomes slow. The result of the physical model on the change of the time at which the magma system is in the rapid cooling stage is shown in Fig.5-1. It is assumed in this model that the melt generated by melting of the roof crust forms one separate layer and the initial magma is divided into several layers at the initial state and that all layers convects vigorously. Cooling from below is not considered. The results suggest that the increase of the number of the double diffusive layer increase the time period of the rapid cooling stage roughly by a factor of the number of the layers. The formation of double diffusive layer causes the time period of the rapid cooling stage and the life-time of the magma with high temperature becomes longer.

The properties of the magma in the slow cooling stage

When the magma cools near or to the EFT of the crust, the magma system enters the slow cooling stage. In order to know the property of the magma in the slow cooling

stage, we have to know the condition of the magma when the temperature of the magma is near or equal to the EFT of the roof crust.

It will be reasonable that the EFT of the crust in the natural system is assumed to be the temperature at which it behaves as liquid by increasing the degree of the partial melting (Huppert and Sparks, 1988b; see §§2). Generally, a partially molten crust and partially crystallized magma have one unique relationship between the temperature and the fraction of the solid phase when the bulk chemical composition is fixed. If no separation of solid and liquid phases occurs in the silicic magma generated by melting of the crust, the silicic magma has the same EFT as the crust. Thus when the silicic magma cools to its EFT, it is solidified by the definition of the EFT. The magma differentiates more or less and hence the EFT of the silicic magma would become lower than that of the crust. Thus I conclude that the property of the magma in the slow cooling stage is approximately determined by the fractionation of the magma generated by melting in and after melting.

There is the exceptional but important case in difference of the above discussion. It is the case that the crust has the eutectic composition in a strict sense. In this case, melting of the crust at the eutectic temperature generate complete liquid. This melt is liquid without solid phases when the system moves the slow cooling stage. Therefore, it is indicated that the magma like this (for example, rhyolitic magma) can be long-lived in the liquid state.

5.2. The effects of the temperature and the compositional variation of the crust.

When the evolution of the magma systems proceeds in the scenario presented in §5.1, the temperature and composition of the crust affect the thermal and compositional evolution of the magma system. I discuss four cases here: (1) the case of the change of the temperature of the roof crust, (2) the case of the change of the composition of the roof crust, (3) the case of the change of the temperature of the floor crust and (4) the case of the change of the composition of the floor crust.

(1) The roof crust

The processes at the roof are important to the thermal history of the magma system. Thus, the effects of the variation of the temperature and the composition of the roof crust are discussed from view point of cooling of the magma. According to the conclusion in §2, when the magma is stagnant or the crust does not melt, cooling of the magma is governed by the temperature of the crust (Case 2 and 3 in Fig.2-4). Thus, consider the case in which the magma is convective and the melting temperature of the roof crust is lower than the temperature of the magma. It is assumed that the temperature at the magma/crust interface is the EFT of the crust.

The effect of the temperature of the roof crust

It is assumed that the conditions except the temperature of the roof crust are the same. The temperature of the roof crust gives little effect on the cooling rate in the rapid cooling stage (Case 1 in Fig.2-4) (Fig.5-2). On the other hand, the maximum amount of the melt generated by melting of the roof crust and the time taken to solidify completely decreases, as the temperature of the roof crust becomes colder (Case 1 in Fig.2-4).

The effect of the composition of the roof crust

It is assumed that the conditions except the composition of the roof crust are the same. The composition of the roof crust determines its EFT. The transition from the rapid cooling stage to the slow cooling stage occurs when the temperature of the magma is near or equal to the EFT of the roof crust. Therefore, as the EFT of the roof crust becomes higher, the transition from the rapid cooling stage to the slow cooling stage occur at higher temperature of the magma (Fig.5-3) and the magma with the higher temperature can be alive in the crust for a long time. On the other hand, the time at which the magma solidifies completely is not affected by the EFT of the roof crust.

(2) The floor crust

The processes at the floor are important to the compositional differentiation of the magma. Thus, the effects of the variation of the temperature and the composition of the floor crust are discussed from view point of compositional differentiation of the magma. The compositional differentiation of the magma is governed by the production rate of the melt of the crust, the intensity of the compositional convection by the instabilities of the melt and the interstitial liquid of the mush and the upward heat flux from the magma to the roof crust. Here, I focus on the production rate of the melt of the floor crust and assume that the other factors are not affected by the change of the condition of the roof crust. Under these strict assumptions, the production rate of the melt is comparable with the rate of the compositional differentiation of the magma. The production rate of the melt at the interface where the temperature is the solidus of the floor crust is regarded as the production rate of the melt of the floor crust.

Since the compositional plume does not carry a heat flux effectively, the heat transfer is almost determined by heat conduction. It is assumed that the heat transfer around the roof of the crust is determined by heat conduction.

The effect of the temperature of the floor crust

It is assumed that the conditions except the temperature of the floor crust are the same. This case is similar to Case 2 in §2. As the temperature of the floor crust becomes colder, the amount of the melt of the floor crust decreases and hence the rate of the fractionation of the basaltic magma decreases (Fig.2-3). It is because the temperature gradient in the floor crust at the interface between the mush and the crust increases as the temperature of the floor crust becomes larger. The heat loss of the magma into the crust increases and the ratio of the heat used to melt the floor crust to the heat to the interface decreases (Fig.5-4).

The effect of the composition of the floor crust

It is assumed that the conditions except the composition of the floor crust are the same. When the composition of the floor crust changes, the change of its solidus and/or

the change of the degree of partial melting of the floor crust in a constant solidus occur. The former case occurs when the system including solid solution and the latter case occurs when the system is the eutectic system. I consider two cases: one is that the solidus of the floor crust changes and the degree of the partial melting does not change and the other is that the solidus does not change and the degree of the partial melting changes.

When the solidus of the floor crust changes, as the solidus of the floor crust is higher, the temperature difference between the magma (or the mush) and the solidus decreases and the temperature difference between the solidus and the far crust. The temperature gradient in the mush at the interface tends to be small while the temperature gradient in the mush at the interface tends to be large (Fig. 5-6a). Therefore, the production rate of the melt decreases and the rate of the chemical differentiation of the magma tends to decrease. The migration of the melting interface is calculated using the model of Case 2 in §2 when the temperature of the magma with 1 km thick is 1200 °C and the initial temperature of the crust is 500 °C. When the solidus of the floor crust is higher than near 850 °C, melting does not occur.

When the degree of partial melting of the floor crust changes (Fig. 5-6b), this case is similar to the analogue experiment in §4.2. As the degree of the partial melting of the crust in its solidus decreases, the production rate of the melt decreases because the temperature gradient in the mush at the interface decreases (see §4.2). Therefore, the rate of the chemical differentiation of the magma tends to decrease.

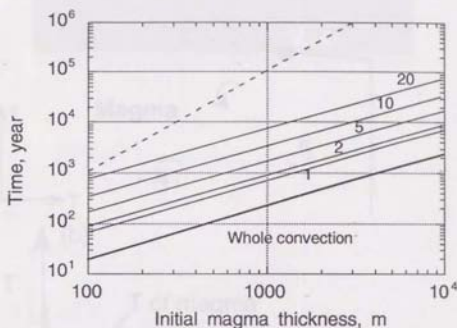


Fig.5-1. The change of the time period of the rapid cooling stage due to the formation of the double diffusive layers in the magma. Solid lines show the time at which the temperature difference between the mean temperature of the magma become 5 % to the temperature difference between the initial temperature of the magma and the melting temperature. The figures besides lines show the number of the layers formed in the original magma. The initial temperature of the magma with 1 km thick is 1200 °C and the initial temperature of the crust is 500 °C.

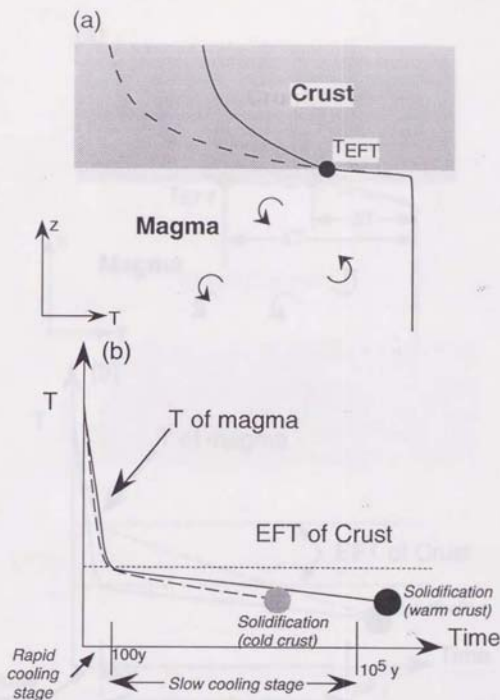


Fig.5-2. The effects of the various temperature of the roof crust. (a) The schematic figure near the interface between the roof crust and the magma. (b) Change of the temperature of the magma. Solid and dashed lines show the cases of the warm and the cold crusts, respectively.

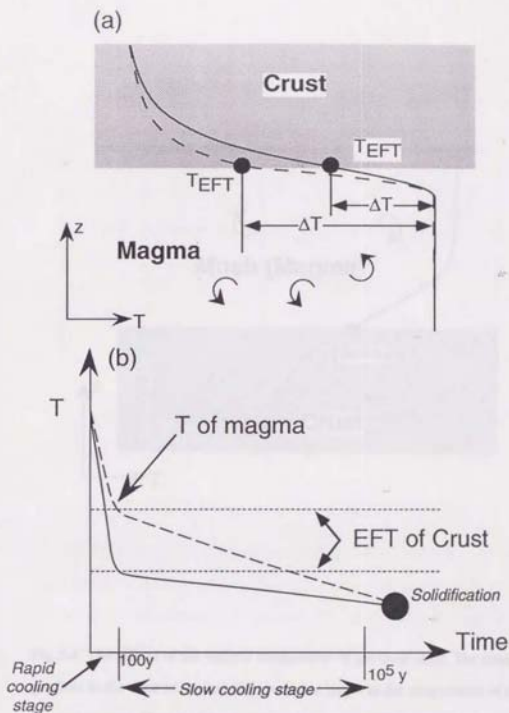


Fig.5-3. The effects of the various composition of the roof crust. The effective fusion temperature of the crust vary according to its composition. (a) The schematic figure near the interface between the roof crust and the magma. (b) Change of the temperature of the magma. Solid and dashed lines show the cases of the warm and the cold crusts, respectively.

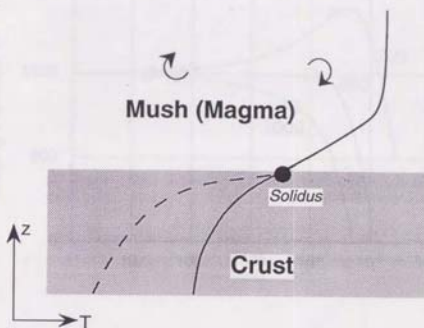


Fig.5-4. The effects of the various temperature of the floor crust. The temperature gradient in the crust at the interface becomes larger as the temperature of the crust becomes colder. Thus the heat loss from the magma into the crust becomes larger as the temperature of the crust becomes colder.

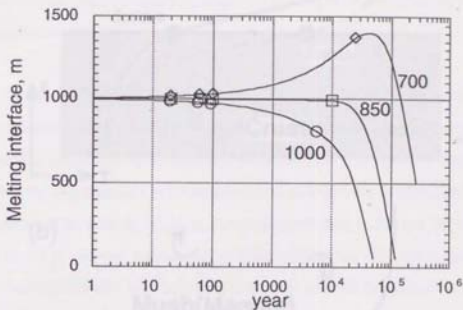


Fig.5-5. Calculation results of the model of Case 2 in §2 in the case of various solidus temperature. The temperature of the magma with 1 km thick is 1200 °C and the initial temperature of the crust is 500 °C. The figures besides line show the solidus temperature (°C)

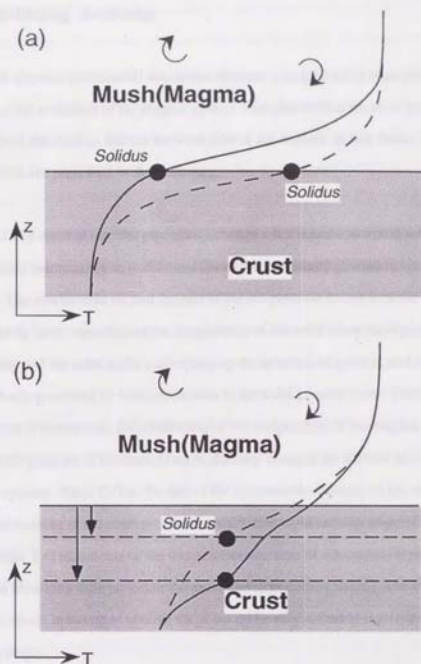


Fig.5-6. The effects of the various temperature of the floor crust. The two cases arise; one is the change of the solidus of the crust, and the other is the change of the degree of partial melting at the solidus. (a) The former case. (b) The latter case.

6. Concluding Remarks

The thermal and material interaction between a magma and a crust give important effects on the evolution of the magma system. I emphasize that we must always consider the effect of the crust to discuss the evolution of the magma. In this thesis, the five conclusions are presented in the following.

(1) The thermal transfer processes between a hot liquid and a cold solid are investigated theoretically to understand the important factors governing cooling of a magma. The results indicate that the rate of the temperature decrease of the liquid is significantly large regardless of the temperature of the solid when the liquid is convective vigorously and the solid melts accompanying the interface migration, and that the liquid cools slowly governed by heat conduction in the solid in other cases. Therefore, when the magma is convective, the relationship of the temperature of the magma (T) and the melting temperature of the crust (T_m) profoundly changes the thermal history of the magma system. When $T > T_m$, the rate of the temperature decrease of the magma is very large and melting of the crust proceeds rapidly (the rapid cooling stage). On the other hand, when $T < T_m$, the rate of the temperature decrease of the magma is small and exists as liquid for a long time period in the crust (the slow cooling stage). The features of the volcanic ejecta in the rapid cooling stage would be very different from that in the slow cooling stage.

(2) A series of the analogue experiments has been carried out using hot solutions and cold solid mixtures of the $\text{NH}_4\text{Cl}-\text{H}_2\text{O}$ binary eutectic system to determine the conditions under which melting and/or convection occur at the roof and the floor of a magma chamber. When a cold solid with the eutectic composition is placed at the top of a hot solution of higher NH_4Cl content, vigorous thermal convection occurs in the solution, which results in rapid melting of the solid roof to form a stable melt layer with negligible mixing of the underlying liquid. On the other hand, when the cold solid mixture is placed at the bottom of the hot solution, the convection is driven by

compositional gradient due to floor melting as well as crystallization just above the floor. Because the compositional convection carries a low heat flux, the rate of melting and the temperature profile around the floor do not differ greatly from those that would be observed due to conduction alone. Unlike the roof melting, the melt generated by the floor melting efficiently mixes with the overlying solution. The compositional gradient generated by the compositional convection enhances the formation of the double diffusive layers in the liquid.

(3) Another series of analogue experiments has been carried out to understand the effects of the compositional and the temperature variation of the floor crust on the evolution of the magma system. The NH_4Cl contents and the initial temperatures of the solid mixtures were systematically changed in the experiments. As the NH_4Cl content of the solid becomes higher, the rate of the compositional differentiation of the liquid decreases. This can be explained by two mechanisms. (1) As the NH_4Cl content of the solid becomes higher, the melting degree of the solid at the solidus becomes smaller and hence the latent heat required by the migration of the interface between the solid and partially molten zone (mush) decreases. Thus, the interface migration becomes faster and hence the temperature gradient just above the interface becomes smaller. These effects result in low heat flux from the mush to the interface and decrease the production rate of the melt with low NH_4Cl content. (2) As the NH_4Cl content of the solid becomes higher, the permeability of the mush becomes smaller. Thus, compositional convection induced by the instability in the mush becomes less vigorous and the liquid of the low NH_4Cl content mixes with the overlying solution less effectively. On the other hand, as the initial temperature of the solid became colder, the rate of the compositional differentiation of the liquid decreases. This is because as the initial temperature of the solid became colder, the heat loss into the solid increases and hence the production rate of the melt of the low NH_4Cl content decreases.

(4) The implication for the thermal and compositional evolution of a magma system is that, when a basaltic magma is emplaced in the continental crust, a silicic magma is rapidly formed by the roof melting, and that the magmas evolve very slowly after the

temperatures of the magmas become as cool as the melting temperature of the crust. The major effects of the floor melting would be that the liquid line of descent of the basaltic magma can be greatly modified by mixing with the melt generated at the floor and the interstitial liquid in the mush and that the upward heat flux decreases due to the formation of the double-diffusive layers.

(5) When the magma system evolves in the scenario described in (3), the variations of the temperature and composition of the crust would affect the evolution of the magma system in the following four points. (i) The temperature of the roof crust gives little effect on the rate of the temperature decrease of the magma in the rapid cooling stage but changes the amount of the melt generated by melting of the roof crust and the cooling of the magma in the slow cooling stage. As the temperature of the roof crust is colder, the amount of the melt generated by roof melting of the crust decreases and the time scale of solidification of the magma becomes shorter. (ii) As the melting temperature of the roof crust becomes higher due to the change in compositions, the transition of the rapid and the slow cooling stages occurs at a higher temperature of the magma. (iii) As the temperature of the floor crust is colder, the amount of the melt generated by melting of the floor crust decreases and hence the rate of the compositional differentiation of the basaltic magma decreases. (iv) When the composition of the floor crust changes, change of its melting temperature and/or change of the degree of partial melting of the crust at the constant melting temperature occur. As the melting temperature of the floor crust becomes higher or as the degree of the partial melting of the crust decreases, then the amount of the melt generated by melting of the floor crust decreases. Therefore, the rate of the compositional differentiation of the basaltic magma decreases.

Improvements in the experiments should be made in the following points to understand the melting and crystallization processes more quantitatively;

(1) Thermal insulation of the experimental system should be improved. The delicate density balances in liquids will determine the formation and extinction of double-diffusive layers and the overturning between the layers. The heat flux from the outside of the

experimental system may affect these processes largely. Experiments should be carried out in a chamber where temperature can be controlled.

(2) In the both sides experiment, after the experimental tank was filled with the liquid above the floor solid, the roof solid was placed in contact with the liquid. Thus the time when the floor solid was in contact with the liquid was earlier by 4 minutes than the time when the roof solid was. This time gap should be smaller or zero.

Important three further problems are brought up to develop quantitative models on the evolution of the magma system;

(1) The formation of the compositional gradient by the compositional convection is important to the formation of the double-diffusive layers. Therefore, it is important to estimate the compositional flux due to melting and crystallization in the mush.

(2) The compositional flux is affected by the temperature profile in the mush, because the temperature profile governs the mass of the melting and crystallization. The heat flux carried by compositional plumes should be estimated. In this thesis, it is relatively small. On the other hand, Some previous papers presented that the heat flux can be effectively carried by the compositional plumes when the density difference due to composition between the melt by the solid and the overlying liquid (e.g. Kerr, 1994).

(3) The upward heat flux is affected by the number of the double-diffusive layers. The number of the double-diffusive layers and its change with time are very important to the thermal history of the system.

Above three problems are not independent ones but their interactions occur. In further investigation, the theoretical model in which the thermal and compositional effects interacts each other. Moreover, it is examined how the processes implicated by this study and further investigations are observed in the natural magma system.

7. Acknowledgements

I would like to acknowledge the continuing guidance and encouragement of Prof. Takehiro Koyaguchi. I wish to express my gratitude to Prof. Toshitsugu Fujii and Dr. Atsushi Yasuda for frequent, stimulating, and helpful discussions. Several helpful discussions with Dr. Jun Oikawa, Miss Mie Ichihara and Dr. Akihiko Tomiya are gratefully acknowledged. Thanks are due to my many colleagues with whom I have discussed this problem. I acknowledge the assistance of Mr. Tetsutaro Asada for fabrication of the experimental apparatus. This work was supported by grants from the Japanese Society for the Promotion of Science and the Ministry of Education, Science, and Culture of the Japanese Government.

8. References

- Bennon, W.D. and Incropera, F.P., 1987a, A continuum model for momentum, heat and species transport in binary solid-liquid phase change systems. 1. Model formulation. *Int. Jour. Heat Mass Transfer*, 30, 2161-2170.
- Bennon, W.D. and Incropera, F.P., 1987b, A continuum model for momentum, heat and species transport in binary solid-liquid phase change systems. 2. Application to solidification in a rectangular cavity. *Int. Jour. Heat Mass Transfer*, 30, 2171-2187.
- Brandeis, G. and Jaupart, C., 1986, On the interaction between convection and crystallization in cooling magma chambers. *Earth Planet. Sci. Lett.*, 345-361.
- Campbell, I.H., 1986, A fluid dynamic model for potholes of the Merensky Reef. *Econo. Geol.* 81, 1181-1125.
- Campbell, I.H. and Turner, J.S., 1987, A laboratory investigation of assimilation at the top of a basaltic magma chamber. *Geology*, 95, 155-172.
- Chemical society of Japan (ed.), 1984, Handbook of Chemistry, Maruzen, in Japanese.
- Chen, C.F. and Chen, F., 1991, Experimental study of directional solidification of aqueous ammonium chloride solution. *Jour. Fluid Mech.*, 227, 567-586
- Chen, C.F. and Turner, J.S., 1980, Crystallization in a double-diffusive system., *Jour. Geoph. Res.*, 74, 7531-7542.
- Chen, F., Yang, T.L., and Lu, J.W., 1993, Influence of convection on solidification of binary solutions cooling from below., *Jour. Appl. Phys.*, 74, 7531-7542.
- Chen, C.F., 1995, Experimental study of convection in a mushy layer during directional solidification. *Jour. Fluid Mech.*, 293, 81-98.
- Huppert, H.E. and Sparks, R.S.J., 1988a, Melting the roof of a chamber containing a hot, turbulently convecting fluid. *Jour. Fluid Mech.*, 188, 107-131.
- Huppert, H.E. and Sparks, R.S.J., 1988b, The generation of granitic magmas by intrusion of basalt into continental crust. *Jour. Petrol.*, 29, 599-624.
- Jaupart, C. and Tait, S., 1995, Dynamics of differentiation in magma reservoirs. *Jour. Geoph. Res.*, 100, 17615-17636.
- Kerr, R.C., 1994, Melting driven by vigorous compositional convection. *Jour. Fluid Mech.*, 280, 255-285.
- Krishnamurti, R., 1968, On the transition to turbulent convection. *Jour. Fluid Mech.*, 42, 295-320.
- Langmuir, C.H., 1989, Geochemical consequences of in situ crystallization. *Nature*, 340, 199-205.
- Marsh, B.D., 1981, On the crystallinity, probability of occurrence and rheology of lavas and magma. *Contrib. Mineral. Petrol.*, 78, 85-98.

- Molen, van der J. and Paterson, M.S., 1979, Experimental deformation of partially-melted granite. *Contrib. Mineral. Petrol.*, 70, 299-318.
- National Astronomical Observatory (ed.), 1993, *Chronological Scientific Tables*, Maruzen, in Japanese.
- Shaw, H.R., 1980, The fracture mechanisms of magma transport from the mantle to the surface. In: Hargreaves, R.B., ed., *Physics of Magmatic Processes*. Princeton University Press 201-64.
- Sparks, R.S.J., Huppert, H.E. and Turner, J.S., 1984, The fluid dynamics of evolving magma chamber. *Phil. Trans. R. Soc. Lond.*, A310, 511-534.
- Tait, S. and Jaupart, C., 1989, Compositional convection in viscous melts. *Nature*, 338, 571-574.
- Tait, S. and Jaupart, C., 1992, Compositional convection in a reactive crystalline mush and melt differentiation. *Jour. Geoph. Res.*, 97, 6735-6756.
- Turner, J.S., 1979, *Buoyancy Effects in Fluids*. Cambridge University Press.
- Turner, J.S. and Campbell, I.H., 1986, Convection and mixing in magma chambers. *Earth-Science Rev.*, 23, 255-352.
- Weast, R.C. (ed.), 1975, *Handbook of Chemistry and Physics*, CRC, Cleveland.
- Woods, A.W., 1991, Fluid mixing during melting. *Phys. Fluids* A3(5), 1393-1404.
- Woods, A.W. and Huppert, H.E., 1989, The growth of compositionally stratified solid above a horizontal boundary. *Jour. Fluid Mech.*, 199, 29-53.
- Worster, M.G., 1986, Solidification of an alloy from a cooled boundary. *Jour. Fluid Mech.*, 167, 481-501.
- Worster, M.G., 1991, Natural convection in a mushy layer. *Jour. Fluid Mech.*, 224, 335-359.
- Washburn, E.W. (ed.), 1929, *International Critical Table*, McGraw-Hill.
- Wickham, S.M., 1987, The segregation and emplacement of granitic magmas. *Jour. Geol. Soc. Lond.*, 144, 281-198.

1848

